Supporting Information

Assessing the Ability of Spectroscopic Methods to Determine the Difference in the Folding Propensities of Highly Similar β-Hairpins

Hanna Andersson,[†] Emma Danelius,[†] Patrik Jarvoll,[†] Stephan Niebling,[†] Ashley J. Hughes,[†] Sebastian Westenhoff, [†] Ulrika Brath,[†] and Máté Erdélyi*[,†,‡]

[†]Department of Chemistry and Molecular Biology, University of Gothenburg, SE-412 96 Gothenburg, Sweden
[‡]The Swedish NMR Centre, SE-413 96 Gothenburg, Sweden

Table of Contents

1 Peptide Synthesis

1.1 Reaction Scheme

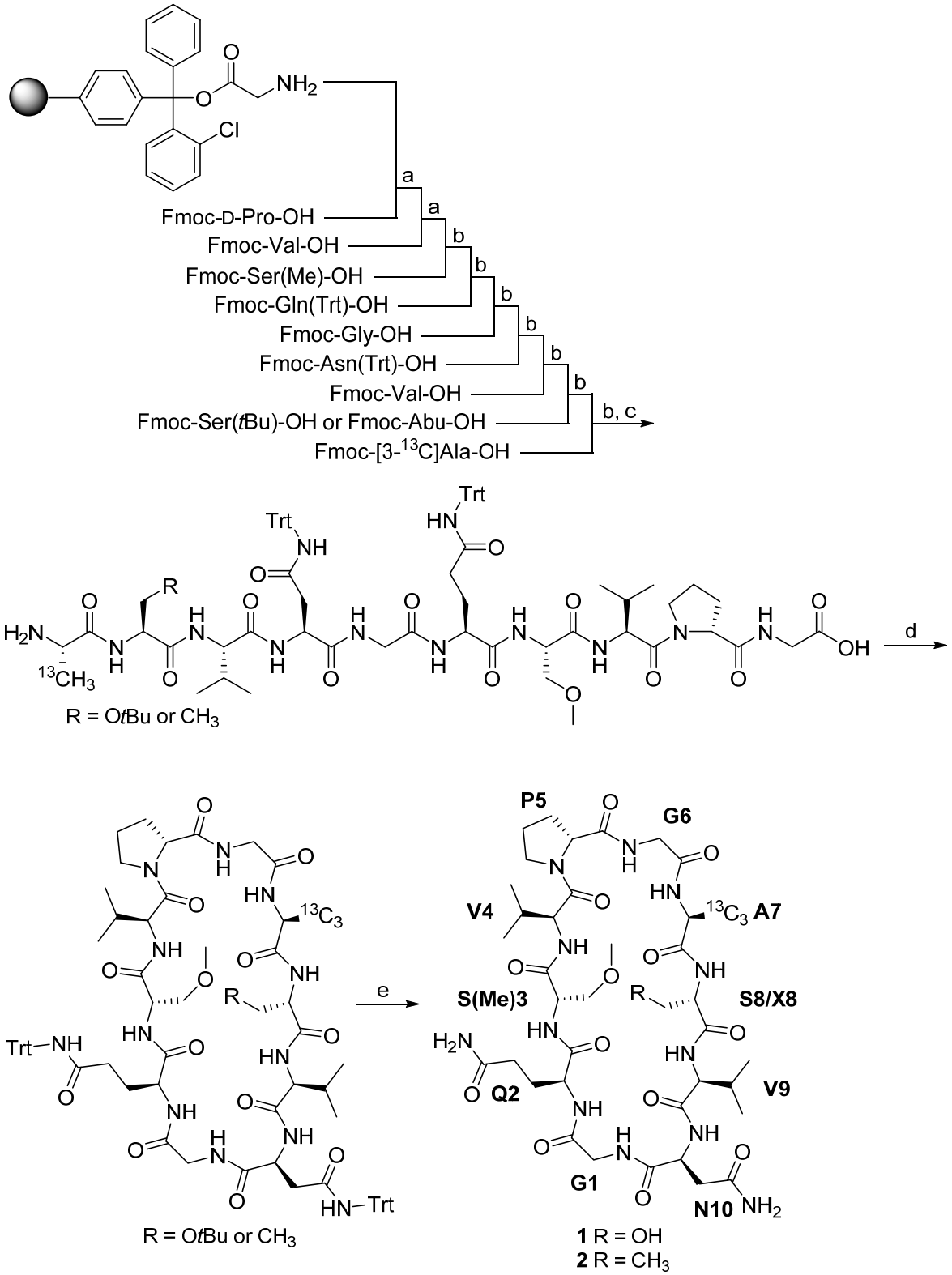

Scheme S1. Reagents and conditions: (a)(i) TBTU, DIPEA, DMF, rt, 2 × 1.5 h, (ii) acetic anhydride, DIPEA, DMF, 20 min, (iii) 20% piperidine/DMF 3 × 5 min; (b) (i) TBTU, DIPEA, DMF, rt, 2 × 1 h, (ii) acetic anhydride, DIPEA, DMF, 20 min, (iii) 20% piperidine/DMF 3 × 5 min; (c)(i) 1% TFA/DCM, 5 × 5 min, (ii) 10% pyridine/CH_3OH; (d) HATU, DIPEA, DMF, on (e) TFA/TIS/H_2O 2–2.5 h.

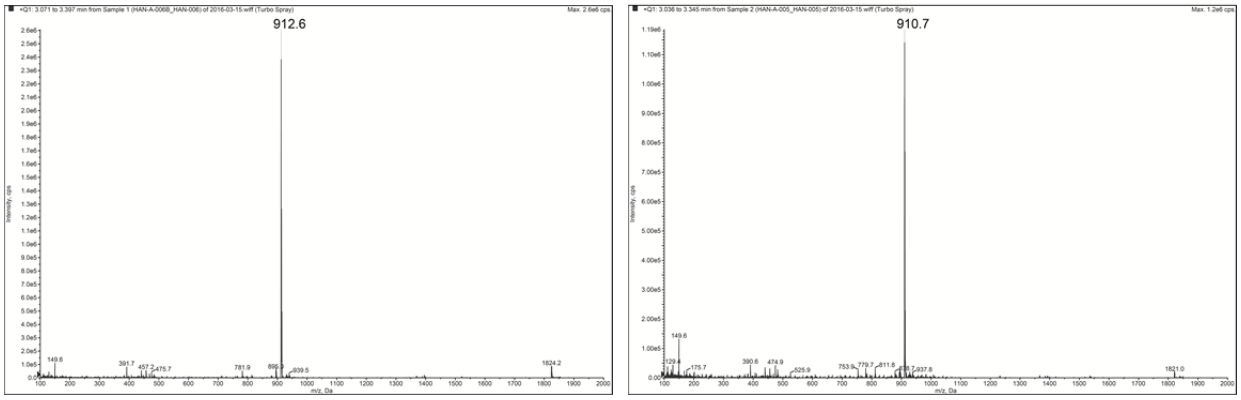

Figure S1. HPLC MS(ESI+) analysis data for peptide **1** (left) and peptide **2** (right).

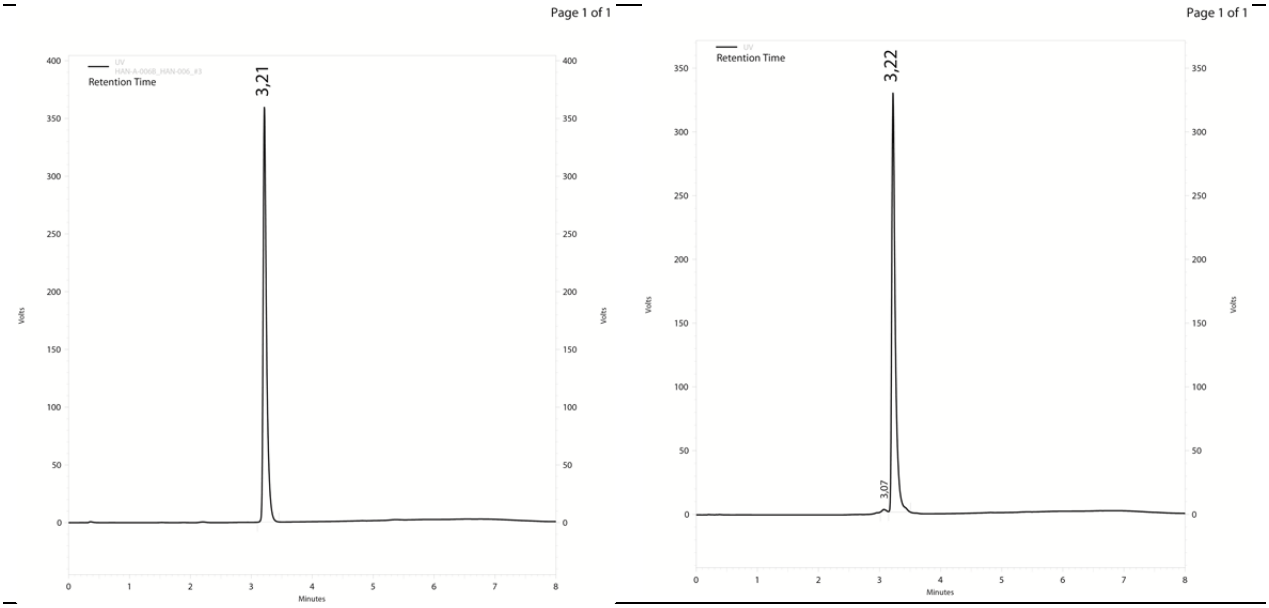

Retention time (min)	Area	Area%
3.21	5457824	>99.9

Retention time (min)	Area	Area%
3.07	50801	1
3.22	5267363	99

Figure S2. HPLC UV analysis data for peptide **1** (left) and peptide **2** (right).

2 NMR Spectroscopy

Both peptide **1** and **2** were confirmed to adopt β-hairpin structures in DMSO-d_6 on the basis of established NMR parameters.[1] The chemical shift dispersion of backbone amide proton resonances, for example, is smaller for unfolded than for folded states due to conformational averaging, and for both **1** and **2** the observed ^{1}HN chemical shift range (7.6–9.4 ppm, Tables S1 and S2) was indicative of folding.[2-3] A $^3J_{HNH\alpha}$ coupling constant larger than 8.0 Hz is typically used as a criterion for identification of β-structures in proteins and peptides. The $^3J_{HNH\alpha}$ coupling constants for both **1** and **2** were ranging from 8.7 to 9.7 Hz for all β-strand residues except S(Me)3 and X8 (Table S3) which provides evidence for β-hairpin formation.[4] For peptides, the application of amide proton temperature coefficients as indicators of NH solvent accessibility and intramolecular hydrogen bonding is limited since they are related to conformational changes as well.[5-6] Exceptions to the general rules of interpretation are often seen and caution is therefore required when drawing any conclusions. With temperature coefficients less negative than -1.4 ppb/K the suggested *i + 3* β-turn residues Q2 and A7 in **1** and **2** (Tables S9 and S10) have a high probability of being hydrogen bonded. β-Turns are key feature of β-structures and in many cases they are found to be stabilized by hydrogen bonds between the *i* (CO) and *i + 3* (NH) residues, just as in **1** and **2**.[7] Secondary structures can also be identified from NOE distance information by visual inspection of NOESY spectra and/or evaluation of NOE derived interproton distances.[8] Antiparallel β-structures are characterized by the presence of repeated short distances (≈2.2 Å) between alpha and amide protons in adjacent strand residues, and this pattern could be identified in both of the peptides ($d_{H\alpha HN}$(2,3; 3,4; 7,8; 8,9; 9,10) = 1.8–1.9 Å, Tables S11 and S12). Another important criterion is the observation of interstrand NOE correlations. The distance derived from the NOE correlation between S(Me)3-Hα and S8/X8-Hα in **1** and **2**, respectively, was found to be 2.2 Å (Tables S11 and S12) which is in agreement with the reference value of 2.3 Å. Overall, the NOE correlations in both of the peptides were consistent with hairpin formation.

2.1 ^{1}H NMR Data

The NMR spectra were recorded at 298.15 K on a 900 MHz spectrometer equipped with a triple-resonance inverse detection cryogenic probe. The protons were assigned from TOCSY and NOESY spectra. The $^{3}J_{HNH\alpha}$ coupling constants were determined from ^{1}H NMR spectra measured on a 400 MHz spectrometer equipped with a double-resonance probe.

Table S1. ^{1}H NMR chemical shift assignment (δ, ppm) for peptide **1** in DMSO-d_6.

Residue	Hα	Hα1	Hα2	Hβ	Hβ1	Hβ2	Hγ	Hγ1	Hγ2	Hδ1	Hδ2	Hε1	Hε2	HN
G1		3.84	3.24											7.98
Q2	4.51				1.86	1.72		2.07	2.02			7.06	6.73	7.57
S(Me)3	4.74				3.56	3.48								8.72
V4	4.28			1.91				0.82	0.77					8.55
^{D}P5	4.28				2.05	1.82		2.06	1.86	3.55	3.49			
G6		3.84	3.41											8.54
A7	4.62				1.29	1.15								7.65
S8/X8	4.84				3.56	3.31								8.34
V9	4.18			1.87				0.82	0.78					8.53
N10	4.07				2.91	2.45				7.38	6.82			9.22

Table S2. ^{1}H NMR chemical shift assignment (δ, ppm) for peptide **2** in DMSO-d_6.

Residue	Hα	Hα1	Hα2	Hβ	Hβ1	Hβ2	Hγ	Hγ1	Hγ2	Hδ1	Hδ2	Hε1	Hε2	HN
G1		3.80	3.23											8.16
Q2	4.55				1.84	1.72		2.08	2.03			7.04	6.72	7.58
S(Me)3	4.81				3.55	3.48								8.78
V4	4.29			1.91				0.82	0.77					8.60
^{D}P5	4.28				2.04	1.83		2.07	1.86	3.56	3.48			
G6		3.85	3.39											8.59
A7	4.62				1.29	1.15								7.63
S8/X8	4.86				1.57	1.35	0.67							8.44
V9	4.21			1.82				0.82	0.78					8.45
N10	4.05				2.92	2.40				7.37	6.81			9.22

Table S3. $^{3}J_{HNH\alpha}$ (Hz) for peptides **1** and **2**.

Residue	Peptide **1**	Peptide **2**
Q2	9.7	9.7
S(Me)3	7.7	7.7
V4	9.7	9.7
A7	9.1	9.3
S8/X8	9.0	7.3
V9	8.9	8.7
N10	7.7	6.1

2.2 ^{15}N NMR Data

The NMR spectra were recorded at 298.15 K on a 900 MHz spectrometer equipped with a triple-resonance inverse detection cryogenic probe. The amide nitrogens were assigned from ^{15}N HSQC spectra.

Table S4. ^{15}N NMR chemical shift assignment (δ, ppm) for peptides **1** and **2** in DMSO-d_6.

Peptide	G1	Q2	S(Me)3	V4	G6	A7	S8/X8	V9	N10
1	102.5	117.0	120.4	123.7	110.4	120.0	117.5	122.1	125.5
2	102.5	116.8	120.5	123.7	110.8	119.9	122.8	121.0	126.6

2.3 ^{13}C NMR Data

The NMR spectra were recorded at 296.15 K on a 800 MHz spectrometer equipped with a triple-resonance carbon-cryogenic probe. The alpha and beta carbons were assigned from gHSQCAD spectra.

Table S5. ^{13}Cα and ^{13}Cβ NMR chemical shift assignment (δ, ppm) for peptides **1** and **2** in DMSO-d_6.

	Peptide **1**		Peptide **2**	
Residue	Cα	Cβ	Cα	Cβ
G1	42.8		43.0	
Q2	50.4	28.9	50.4	29.3
S(Me)3	52.7	70.9	52.8	71.0
V4	55.7	29.7	55.6	29.8
^{D}P5	59.9	28.2	59.9	28.2
G6	42.5		42.6	
A7	46.5	19.3	46.5	19.5
S8/X8	54.1	61.5	53.3	25.6
V9	57.5	30.9	57.2	31.6
N10	50.9	35.4	51.0	35.3

2.4 $^{13}C\beta$ and $^{13}C\alpha$ Structuring Shifts

Structuring shifts, which are also referred to as conformational shifts and chemical shift deviations (CSDs), are frequently used for both qualitative and quantitative assessment of β-hairpin folding and are defined as the difference between observed chemical shifts and the corresponding random coil chemical shifts ($\Delta\delta = \delta_{obs} - \delta_{random\ coil}$).[2, 9] In the last decade it has been found that only the cross-strand hydrogen bonded residues are suitable for CSD analysis of β-hairpins, and that $^{13}C\beta$ CSDs are more useful than $^{13}C\alpha$ CSDs for elucidating β-structures.[10] It is known that $^{13}C\beta$ CSDs are positive and that $^{13}C\alpha$ CSDs are negative for strand β-hairpin residues, whereas at least one of the β-turn residues display a negative $^{13}C\beta$ CSD value and a positive $^{13}C\alpha$ CSD value.[9, 11] As shown in Tables S6 and S7, and Figures S1 and S2, these trends were observed for the hydrogen bonded and the turn residues in both **1** and **2**, a result indicating that they adopt β-hairpin structures in DMSO-d_6 at 306.60 and 306.85 K, respectively. The fact that only one anomalous value was obtained in the $^{13}C\beta$ and $^{13}C\alpha$ CSD analyses (V4 and V9, respectively) indicates that the folded population for **1** and **2** are large.[11]

Table S6. $^{13}C\beta$ CSDs ($\Delta\delta$, ppm) for peptides **1** and **2** in DMSO-d_6.

		Peptide **1**			Peptide **2**		
Residue	Type	δ_{obs} [a]	$\delta_{random\ coil}$ [c]	$\Delta\delta$	δ_{obs} [b]	$\delta_{random\ coil}$ [c]	$\Delta\delta$
Q2	HB strand	28.88	27.64	1.24	29.37	27.64	1.73
S(Me)3	NHB strand		NA			NA	
V4	HB strand	29.74	30.54	–0.80[d]	29.84	30.54	–0.70[d]
^{D}P5	Turn	28.22	28.74[e]	–0.52	28.20	28.74[e]	–0.54
A7	HB strand	19.23	17.94	1.29	19.41	17.94	1.47
S8/X8	NHB strand	61.54	61.30	0.20		NA	
V9	HB strand	30.88	30.54	0.34	31.57	30.54	1.03
N10	Turn	35.51	36.84	–1.33	35.38	36.84	–1.46

NA, not available. HB, Hydrogen bonded. NHB, Non-hydrogen bonded.

[a]Indirectly referenced to TMS via the DMSO-d_6 residual signal.[12] $\delta_{DMSO\text{-}d6}$ at 306.60 K = 39.52 ppm. [b]Indirectly referenced to TMS via the DMSO-d_6 residual signal.[12] $\delta_{DMSO\text{-}d6}$ at 306.85 K = 39.52 ppm. [c]Data from Grathwohl and Wüthrich[13] were referenced according to Hoffman and Davies,[12] i.e. corrected by –0.26 ppm ($\Delta\delta_{DMSO\text{-}d6}$ at 308.15 K = 39.80–39.54 ppm). [d]Anomalous value (i.e. sign opposite to that characteristic of a strand residue). [e]$\delta_{random\ coil}$ for *trans* proline was used.

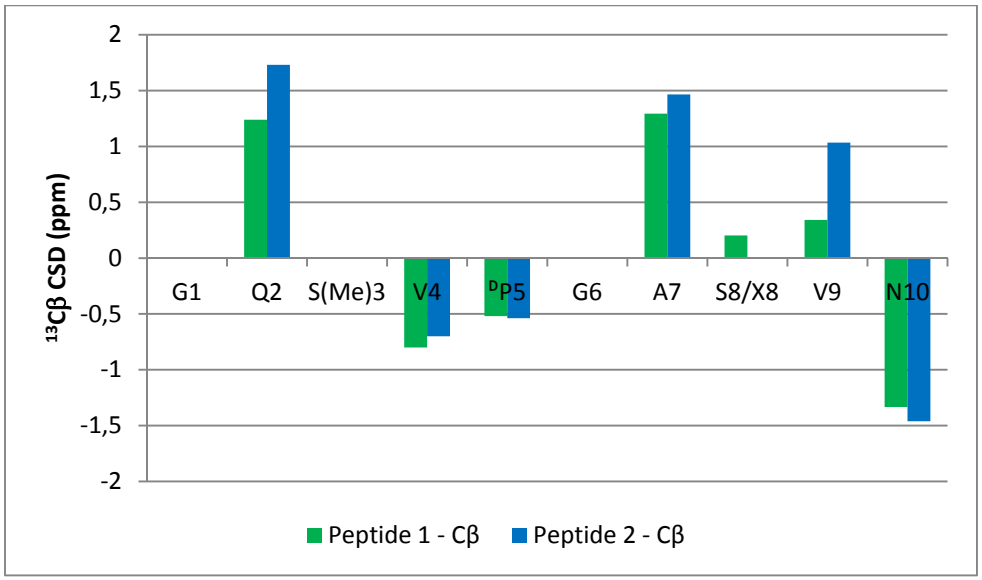

Figure S3. $^{13}C\beta$ chemical shift deviation (CSD) histograms for peptides **1** ad **2**. The random coil chemical shift for *trans* proline was used for ^{D}P5. No random coil chemical shifts were available for S(Me)3 and X8. Anomalous values were obtained for V4 (i.e. i.e. sign opposite to that characteristic of a strand residue). The G1 and G6 residues does not have any beta carbons.

Table S7. $^{13}C\alpha$ CSDs ($\Delta\delta$, ppm) for peptides **1** and **2** in DMSO-d_6.

		Peptide **1**			Peptide **2**		
Residue	Type	δ_{obs} [a]	$\delta_{random\ coil}$ [c]	$\Delta\delta$	δ_{obs} [b]	$\delta_{random\ coil}$ [c]	$\Delta\delta$
G1	Turn	42.84	41.84	1.00	42.98	41.84	1.14
Q2	HB strand	50.50	51.44	−0.94	50.46	51.44	−0.98
S(Me)3	NHB strand		NA			NA	
V4	HB strand	55.74	56.74	−1.00	55.67	56.74	−1.07
^{D}P5	Turn	59.93	58.84[d]	1.09	59.93	58.84[d]	1.09
G6	Turn	42.56	41.84	0.72	42.61	41.84	0.77
A7	HB strand	46.64	47.74	−1.10	46.59	47.74	−1.15
S8/X8	NHB strand	54.10	54.50	−0.44		NA	
V9	HB strand	57.58	56.74	0.84[e]	57.29	56.74	0.55[e]
N10	Turn	50.97	49.04	1.93	51.01	49.04	1.97

NA, not available. HB, Hydrogen bonded. NHB, Non-hydrogen bonded.

[a]Indirectly referenced to TMS via the DMSO-d_6 residual signal.[12] $\delta_{DMSO\text{-}d6}$ at 306.60 K = 39.52 ppm. [b]Indirectly referenced to TMS via the DMSO-d_6 residual signal.[12] $\delta_{DMSO\text{-}d6}$ at 306.85 K = 39.52 ppm. [c]Data from Grathwohl and Wüthrich[13] were referenced according to Hoffman and Davies,[12] i.e. corrected by −0.26 ppm ($\Delta\delta_{DMSO\text{-}d6}$ at 308.15 K = 39.80−39.54 ppm). [d]$\delta_{random\ coil}$ for trans proline was used. [e]Anomalous value (i.e. sign opposite to that characteristic of a strand residue).

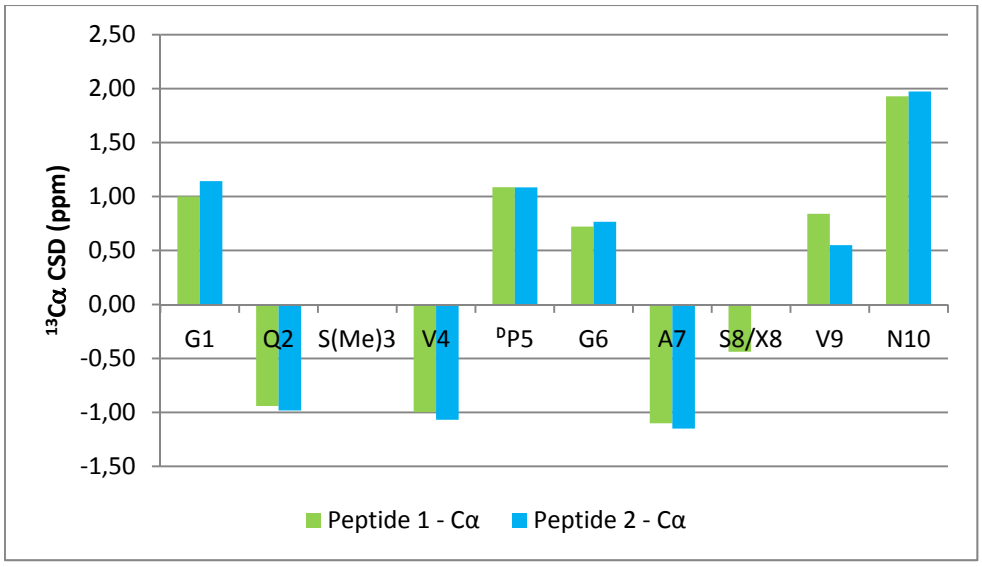

Figure S4. Histograms showing $^{13}C\alpha$ CSDs for the amino acid residues of peptides **1** and **2**. The random coil chemical shift for *trans* proline was used for ^{D}P5. No random coil chemical shifts were available for S(Me)3 and X8. Anomalous values were obtained for V9 (i.e. sign opposite to that characteristic of a strand residue).

2.5 Variable Temperature ^{13}C NMR Data — A7-^{13}Cβ Detection

The NMR studies were carried out at 298.98–403.83 K, with $\Delta T = 4$ or 5 K, using a 500 MHz spectrometer equipped with a triple-resonance probe. The two peptides were analyzed simultaneously using a spinner which can accommodate two 2.5 mm tubes.

Table S8. Variable temperature chemical shifts (δ, ppm) for peptides **1** and **2** in DMSO-d_6.

T (K)	Peptide **1**	Peptide **2**	*T* (K)	Peptide **1**	Peptide **2**
298.98	19.38	19.52	354.43	18.86	19.09
304.02	19.34	19.49	359.47	18.80	19.04
309.06	19.31	19.46	364.51	18.76	19.01
314.10	19.27	19.42	369.55	18.68	18.93
319.14	19.22	19.39	374.60	18.61	18.87
324.19	19.18	19.35	379.64	18.55	18.81
329.23	19.13	19.31	384.68	18.48	18.75
334.27	19.08	19.27	389.72	18.41	18.68
339.31	19.03	19.23	394.76	18.35	18.63
344.35	18.98	19.18	399.80	18.28	18.57
349.39	18.92	19.14	403.83	18.23	18.52

2.6 Variable Temperature ^{13}C NMR Data — ^{13}Cα and ^{13}Cβ Detection

The NMR studies were carried out at 296.15–343.15 K, with $\Delta T \approx 5$ K, using a 800 MHz spectrometer equipped with a triple-resonance carbon-cryogenic probe. The superimposed VT ^{13}C NMR spectra covering the aliphatic carbons of **1** and **2**, respectively, are presented in Figures S3–S5. The peaks are colored blue-orange-yellow-purple-green-cyan-red-blue-orange-yellow-purple going from the lowest to the highest temperatures.

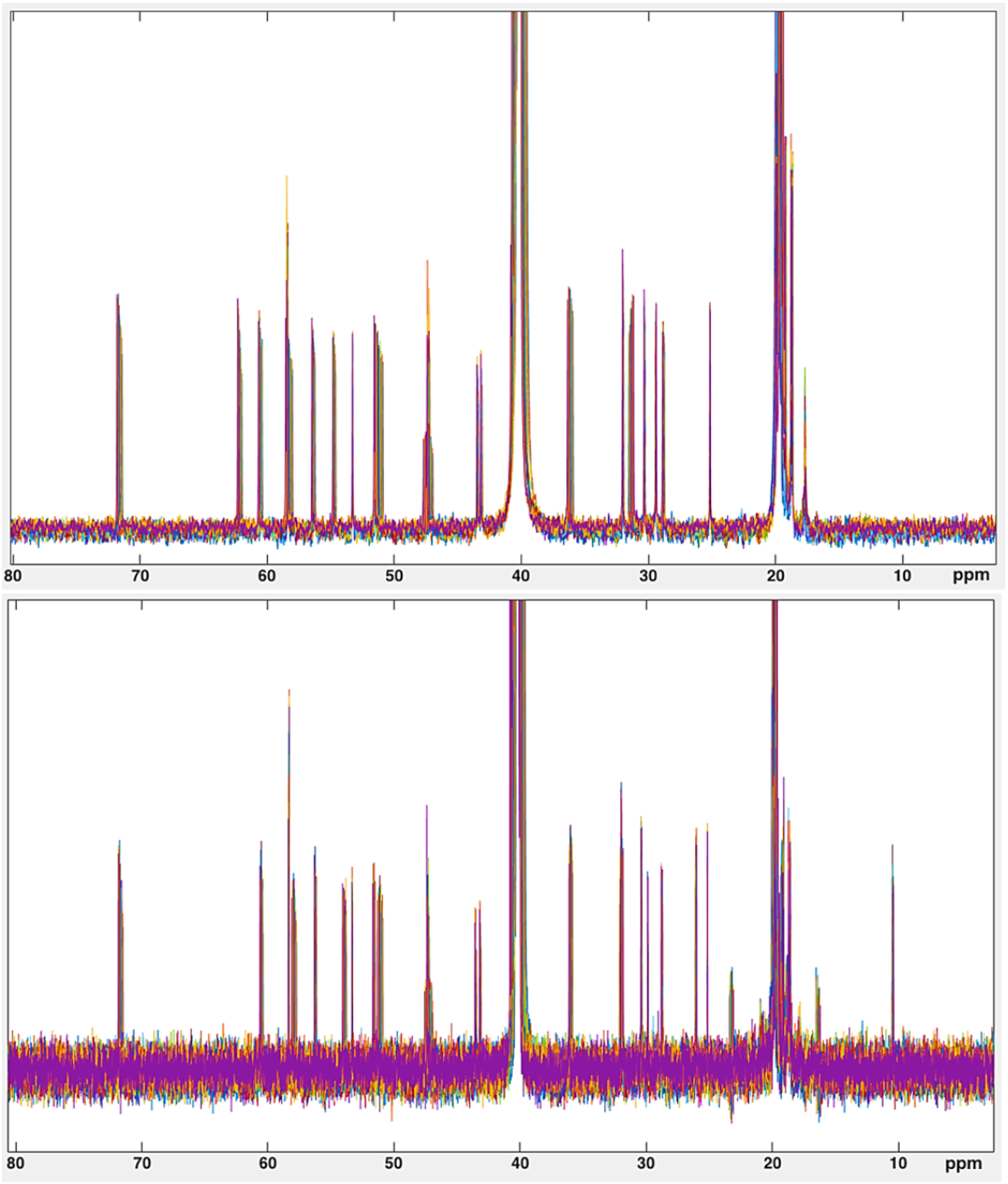

Figure S5. Superimposed ^{13}C NMR spectra for peptide **1** (top) and **2** (bottom) at various temperatures, with the aliphatic chemical shift region being shown.

S(Me)3-Cβ

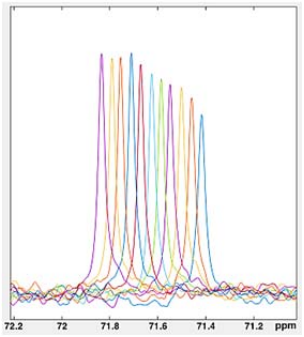

S8-Cβ and ^{D}P5-Cα

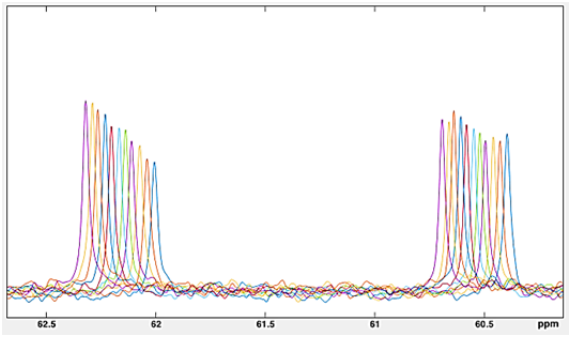

S(Me)3-Cδ and V9-Cα

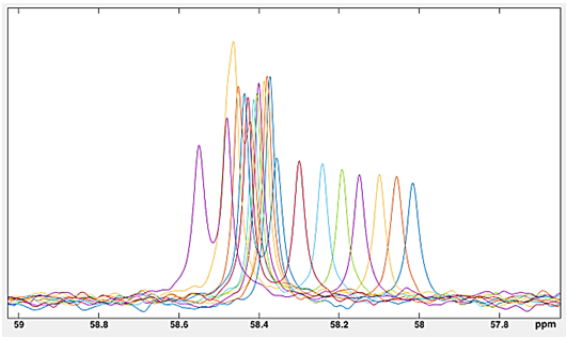

V4-Cα, S8-Cα and S(Me)3-Cα

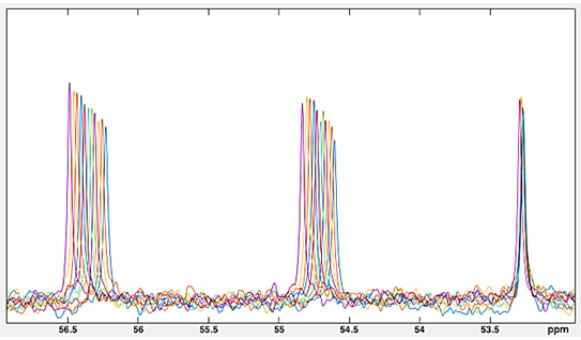

N10-Cα and Q2-Cα

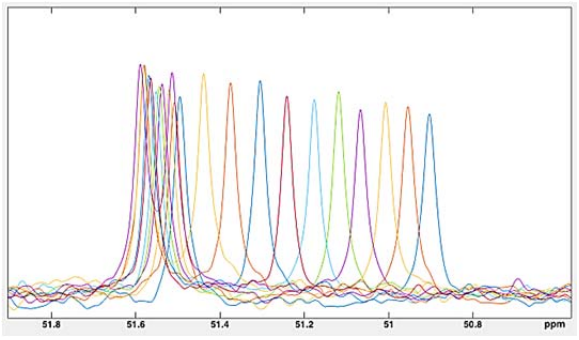

^{D}P5-Cδ and A7-Cα

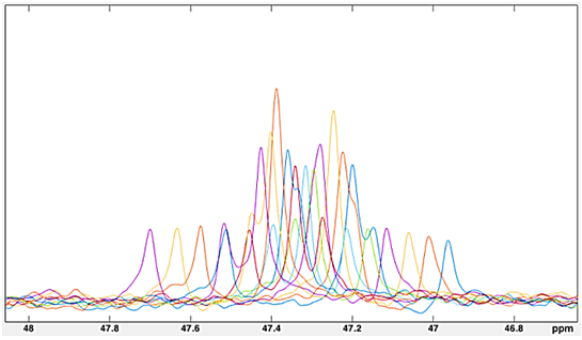

G1-Cα and G6-Cα

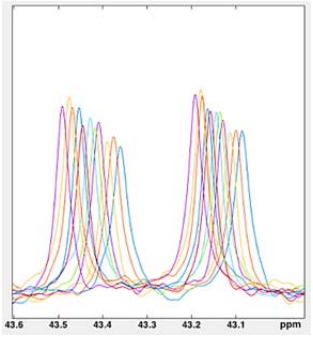

N10-Cβ

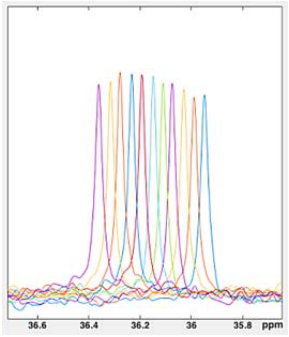

V9-Cβ

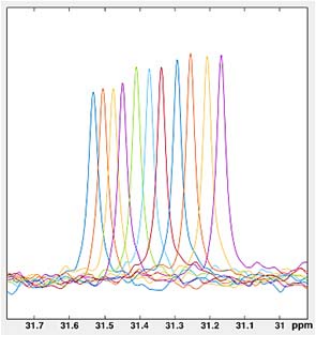

V4-Cβ, Q2-Cβ and ^{D}P5-Cβ

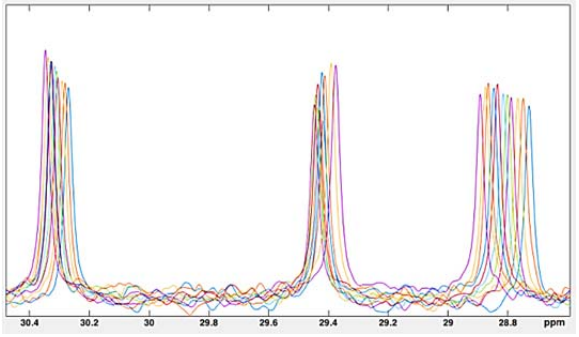

A7-^{13}Cβ

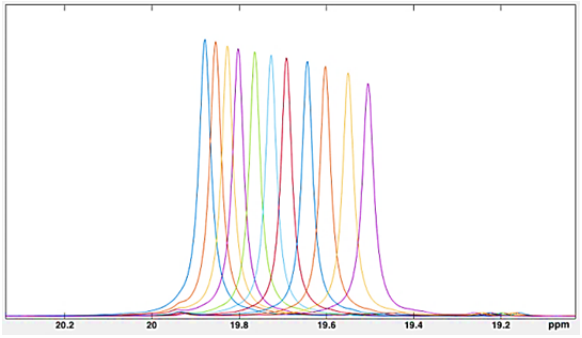

Figure S6. Chemical shift regions of the superimposed VT ^{13}C NMR spectra for peptide **1** covering the alpha and beta carbons.

S(Me)3-Cβ

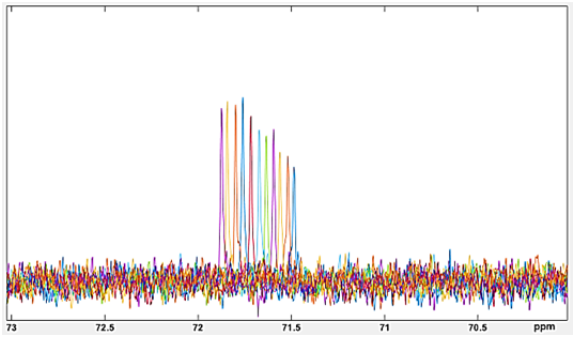

^{D}P5-Cα

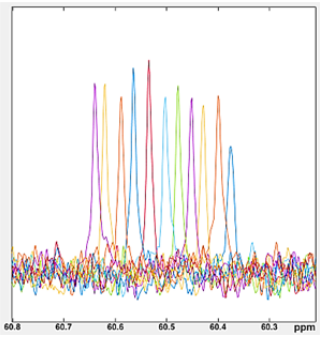

V9-Cα and V4-Cα

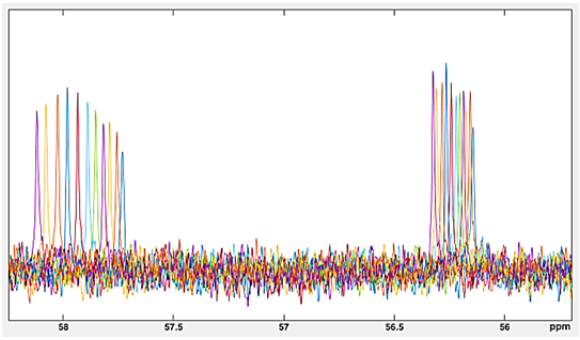

X8-Cα and S(Me)3-Cα

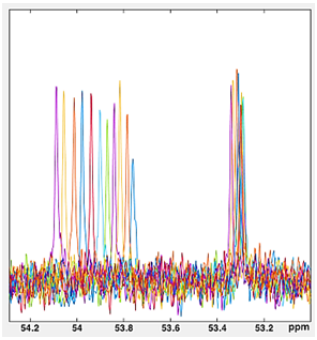

N10-Cα and Q2-Cα

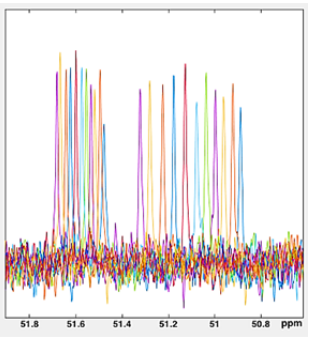

^{D}P5-Cδ and A7-Cα

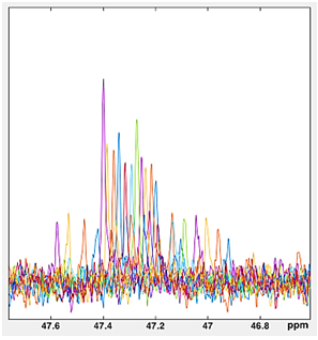

G1-Cα and G6-Cα

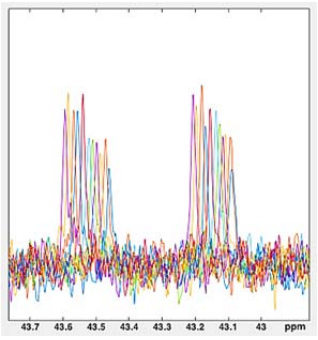

N10-Cβ

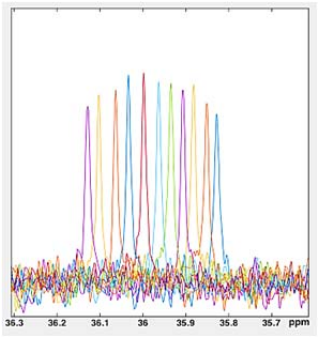

V9-Cβ and Q2-Cγ

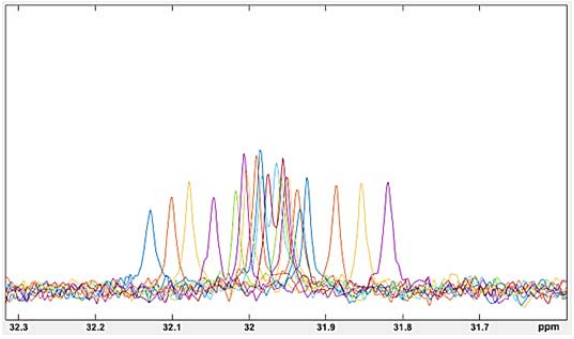

V4-Cβ and Q2-Cβ

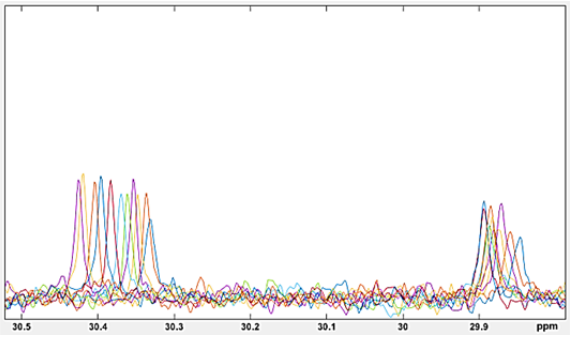

^{D}P5-Cβ

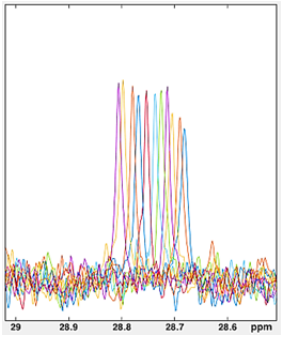

X8-Cβ

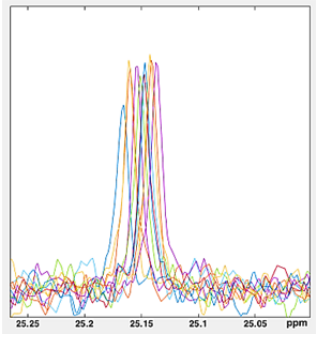

A7-^{13}Cβ

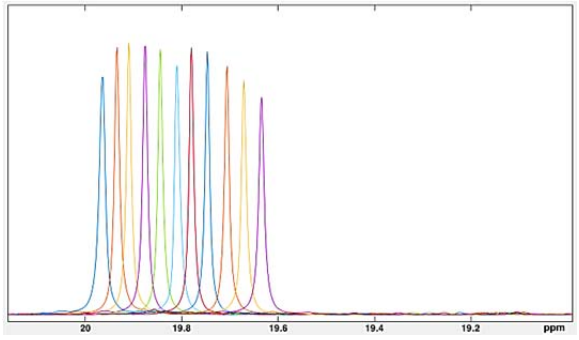

Figure S7. Chemical Shift regions of the superimposed VT ^{13}C NMR spectra for peptide **2** covering the alpha and beta carbons.

2.7 Amide Proton Temperature Coefficients

Amide temperature coefficients ($\Delta\delta_{NH}/\Delta T = (\delta_{T\,high}-\delta_{T\,low})/(T_{high}-T_{low})$) were determined from ^{1}H NMR spectra recorded at 338.15–363.15 K ($\Delta T = 5$ K) on a 500 MHz spectrometer equipped with a triple-resonance probe.

Table S9. Amide proton temperature coefficients $\Delta\delta_{NH}/\Delta T$ (ppb/K) in DMSO-d_6 for peptide **1**.

T (K)	G1	Q2	S(Me)3	V4	A7	S8	N10
338.15	7.76	7.52	8.47	8.37	7.63	8.09	8.85
343.15	7.74	7.52	8.44	8.35	7.62	8.06	8.80
348.15	7.72	7.51	8.40	8.32	7.62	8.03	8.75
353.15	7.70	7.51	8.37	8.29	7.62	8.00	8.70
358.15	7.68	7.50	8.33	8.26	7.62	7.97	8.65
363.15	7.66	7.49	8.29	8.23	7.61	7.94	8.59
$\Delta\delta_{NH}$	−0.11	−0.03	−0.18	−0.15	−0.02	−0.15	−0.26
$\Delta\delta_{NH}/\Delta T$	−4.2	**−1.2**	−7.3	−5.9	**−0.6**	−6.0	−10.4

Table S10. Amide proton temperature coefficients $\Delta\delta_{NH}/\Delta T$ (ppb K^{-1}) in DMSO-d_6 for peptide **2**.

T (K)	G1	Q2	S(Me)3	V4	A7	X8	N10
338.15	7.93	7.53	8.55	8.48	7.59	8.20	8.94
343.15	7.90	7.52	8.52	8.46	7.59	8.17	8.90
348.15	7.87	7.52	8.49	8.44	7.58	8.14	8.86
353.15	7.85	7.51	8.46	8.41	7.58	8.11	8.82
358.15	7.82	7.50	8.42	8.39	7.57	8.08	8.78
363.15	7.79	7.50	8.39	8.37	7.57	8.05	8.74
$\Delta\delta_{NH}$	−0.14	−0.03	−0.16	−0.11	−0.02	−0.15	−0.21
$\Delta\delta_{NH}/\Delta T$	−5.6	**−1.4**	−6.6	−4.5	**−0.9**	−6.0	−8.4

2.8 NOE Build-Up Analysis

NOESY spectra were recorded at 298.15 K on a 900 MHz NMR spectrometer. NOE build-ups were recorded without solvent suppression with mixing times of 100, 200, 400, 500, 600 and 700 ms.

Table S11. Interproton distances (Å) for peptide **1** derived from NOE build-up measurements. Geminal protons N10-Hβ1 and N10-Hβ2 were used as reference (1.78 Å).

No.	Protons		Buildup Coefficient (σ)	R^2	Experimental distance (Å)
1	N10-HN	Q2-HN	0.000012418	0.99	3.26
2	N10-HN	G1-HN	0.000096338	1.00	2.32
3	N10-HN	V9-Hα	0.000406355	1.00	1.82
4	S(Me)3-HN	Q2-HN	0.000025316	0.98	2.90
5	S(Me)3-HN	Q2-Hα	0.000389592	1.00	1.84
6	S(Me)3-HN	V4-HN	0.000020048	0.99	3.01
7	S(Me)3-HN	S8-Hα	0.000008680	0.98	3.46
8	V4-HN	S(Me)3-Hα	0.000347396	1.00	1.87
9	G6-HN	A7-HN	0.000127844	1.00	2.21
10	V9-HN	G1-HN	0.000021284	1.00	2.98
11	V9-HN	S8-Hα	0.000376906	1.00	1.85
12	V9-HN	S8-HN	0.000026407	0.98	2.88
13	S8-HN	A7-HN	0.000024615	0.99	2.91
14	S8-HN	A7-Hα	0.000320997	1.00	1.90
15	S8-HN	S(Me)3-Hα	0.000010308	0.99	3.37
16	G1-HN	Q2-Hα	0.000011594	0.99	3.30
17	G1-HN	S8-Hα	0.000008311	0.98	3.49
18	G1-HN	N10-Hα	0.000120589	1.00	2.23
19	G1-HN	V9-Hα	0.000027129	0.99	2.86
20	G1-HN	Q2-HN	0.000133569	1.00	2.20
21	A7-HN	S(Me)3-Hα	0.000013366	0.98	3.22
22	A7-HN	S8-Hα	0.000006220	0.99	3.66
23	Q2-HN	V9-Hα	0.000009248	0.98	3.43
24	Q2-HN	S(Me)3-Hα	0.000006257	0.99	3.66
25	Q2-HN	S8-Hα	0.000024686	0.98	2.91
26	Q2-HN	N10-Hα	0.000013040	0.99	3.24
27	S8-Hα	S(Me)3-Hα	0.000139095	1.00	2.18
28	S8-Hα	A7-Hα	0.000014518	0.99	3.18
29	S8-Hα	Q2-Hα	0.000003322	0.98	4.06
30	S(Me)3-Hα	Q2-Hα	0.000020653	0.98	3.00
31	N10-Hβ1	N10-Hβ2	0.000471160	1.00	1.78

Figure S8. NOE build-up curves (1–31) for peptide **1**.

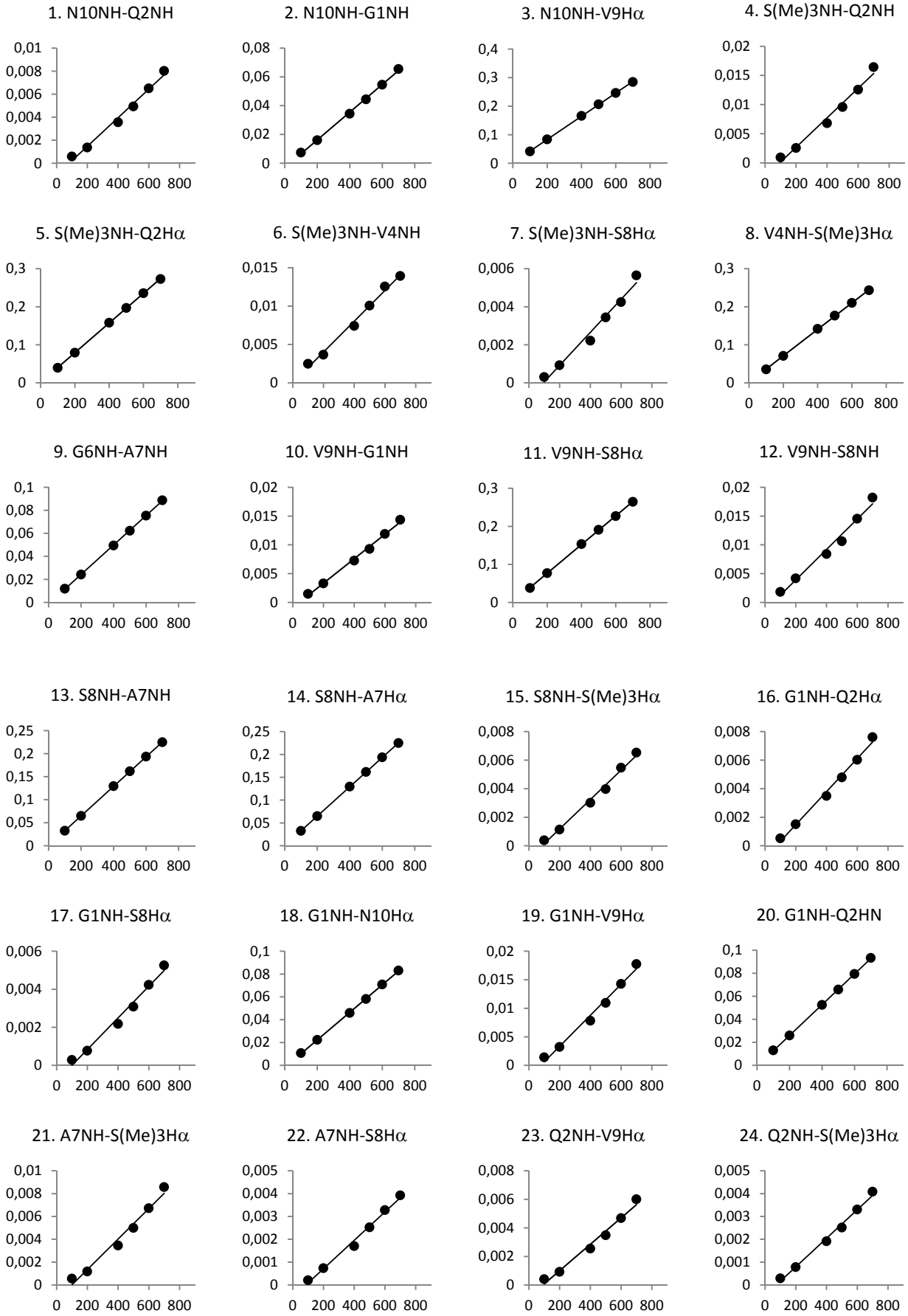

25. Q2NH-S8Hα

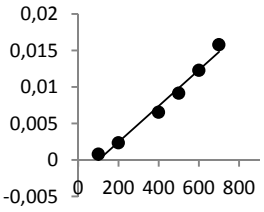

26. Q2NH-N10Hα

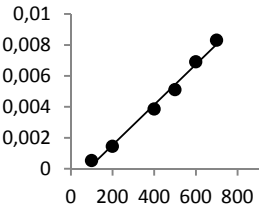

27. S8Hα-S(Me)3Hα

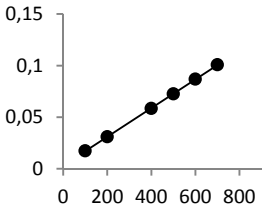

28. S8Hα-A7Hα

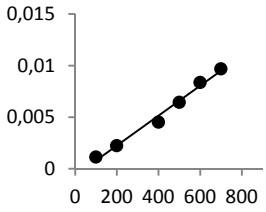

29. S8Hα-Q2Hα

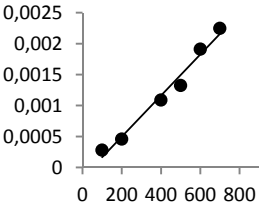

30. S(Me)3Hα-Q2Hα

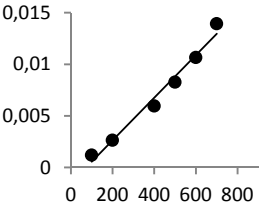

31. N10Hβ1-N10Hβ2

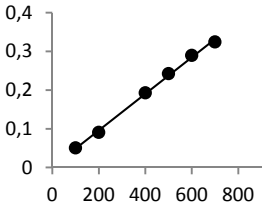

Table S12. Interproton distances (Å) for peptide **2** derived from NOE build-up measurements. Geminal protons N10-Hβ1 and N10-Hβ2 were used as reference (1.78 Å).

No.	Protons		Buildup Coefficient (σ)	R^2	Experimental distance (Å)
1	N10-HN	G1-HN	9.19577E-05	1.00	2.28
2	N10-HN	V9-Hα	0.000414859	1.00	1.78
3	N10-HN	Q2-HN	1.20823E-05	0.99	3.20
4	N10-HN	V9-HN	2.1977E-05	0.99	2.90
5	S(Me)3-HN	X8-Hα	1.09526E-05	0.98	3.25
6	S(Me)3-HN	Q2-Hα	0.000367216	1.00	1.81
7	S(Me)3-HN	V4-HN	1.88824E-05	0.98	2.97
8	S(Me)3-HN	Q2-HN	2.03523E-05	0.98	2.93
9	S(Me)3-HN	V9-HN	5.32396E-06	0.98	3.67
10	V4-HN	S(Me)3-Hα	0.000351431	1.00	1.83
11	V4-HN	V9-HN	2.12843E-05	0.98	2.91
12	V4-HN	X8-Hα	7.15285E-05	1.00	2.38
13	V4-HN	A7-Hα	9.37298E-06	0.98	3.34
14	G6-HN	A7-HN	0.000133345	1.00	2.15
15	G6-HN	^{D}P5-Hα	0.000218194	1.00	1.98
16	V9-HN	S(Me)3-Hα	5.17488E-05	0.99	2.51
17	V9-HN	X8-Hα	0.000428596	1.00	1.77
18	V9-HN	Q2-Hα	7.96155E-06	0.99	3.43
19	V9-HN	Q2-HN	7.31849E-05	1.00	2.37
20	V9-HN	G1-HN	1.44951E-05	1.00	3.11
21	X8-HN	A7-HN	1.53209E-05	0.99	3.08
22	X8-HN	A7-Hα	0.000281806	1.00	1.89
23	G1-HN	V9-Hα	2.4608E-05	0.99	2.84
24	G1-HN	N10-Hα	0.000124374	1.00	2.17
25	G1-HN	Q2-HN	0.000106687	1.00	2.23
26	A7-HN	S(Me)3-Hα	1.13309E-05	0.98	3.24
27	A7-HN	X8-Hα	5.31292E-06	0.98	3.67
28	Q2-HN	V9-Hα	9.10877E-06	0.98	3.36
29	Q2-HN	N10-Hα	1.19789E-05	0.99	3.21
30	Q2-HN	S(Me)3-Hα	6.18632E-06	0.98	3.58
31	Q2-HN	X8-Hα	2.30687E-05	0.98	2.87
32	X8-Hα	S(Me)3-Hα	0.000133192	1.00	2.15
33	S(Me)3-Hα	Q2-Hα	1.8607E-05	0.98	2.98
34	N10-Hβ1	N10-Hβ2	0.000408596	1.00	1.78

Figure S9. NOE build-up curves (1–34) for peptide **2**.

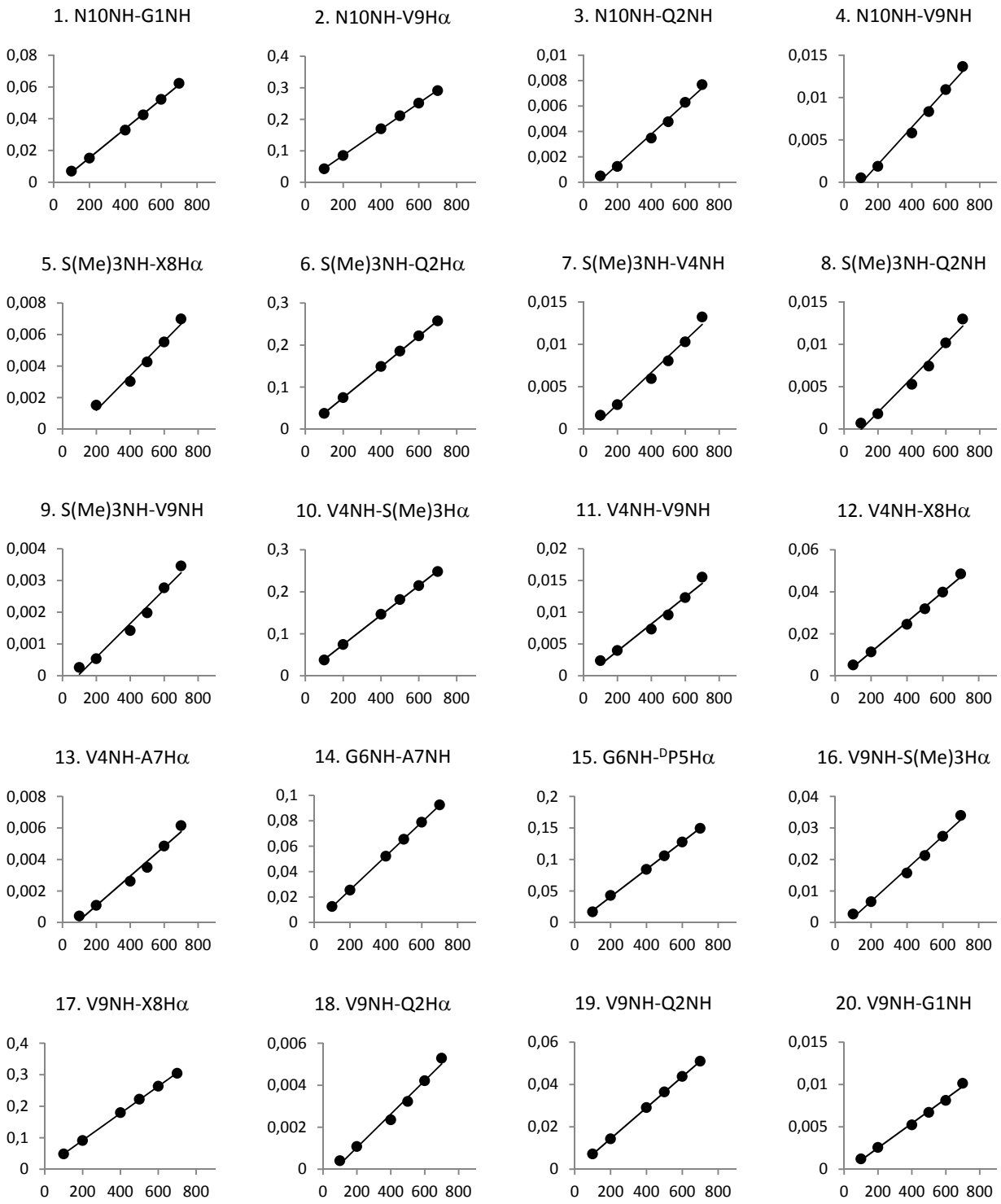

21. X8NH-A7NH

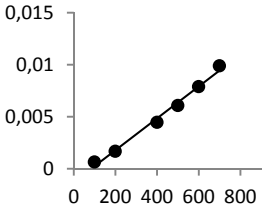

22. X8NH-A7Hα

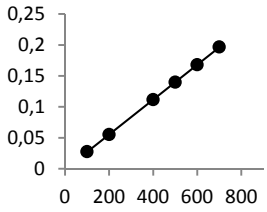

23. G1NH-V9Hα

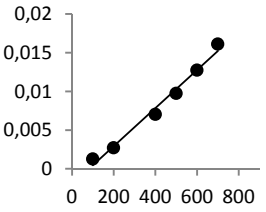

24. G1NH-N10Hα

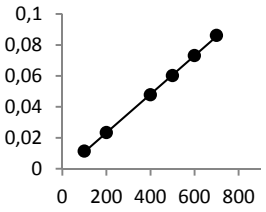

25. G1NH-Q2NH

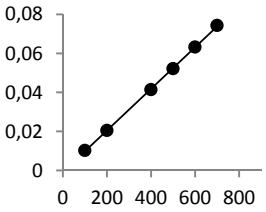

26. A7NH-S(Me)3Hα

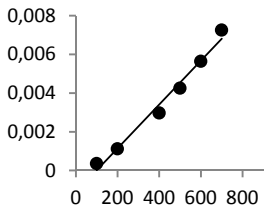

27. A7NH-X8Hα

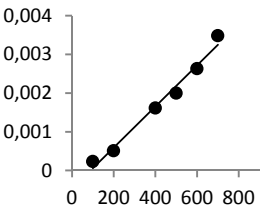

28. Q2NH-V9Hα

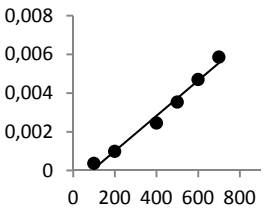

29. Q2NH-N10Hα

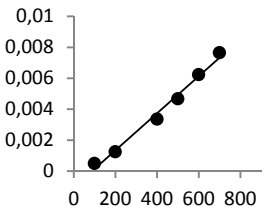

30. Q2NH-S(Me)3Hα

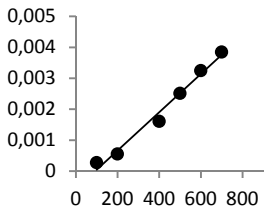

31. Q2NH-X8Hα

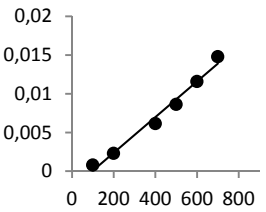

32. X8Hα-S(Me)3Hα

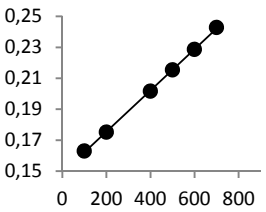

33. S(Me)3Hα-Q2Hα

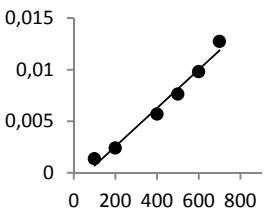

34. N10Hβ1-N10Hβ2

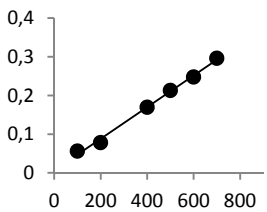

3 Computational Conformational Analysis

Preferred low energy conformations for **1** and **2** were generated by Monte Carlo conformational searching followed by energy minimization and clustering analysis in order to eliminate redundant conformations.

Table S13. Results of the conformational analysis.

			Number of conformations		
Peptide	Force filed	Total[a]	Within 12.6 kJ/mol[b]	Within 42.0 kJ/mol[c]	After clustering analysis[d]
1	OPLS	324	30	324	80
	Amber*	182	6	181	
2	OPLS	297	26	297	147
	Amber*	295	24	295	

[a]Total number of unique conformations found. [b]Conformations found within 12.6 kJ/mol (3.0 kcal/mol) of the global minimum. [c]Conformations found within 42.0 kJ/mol (10.0 kcal/mol) of the global minimum. [d]Conformations obtained after redundant conformation elimination with a 2.5 Å root-mean-square deviation cutoff for heavy atoms. This conformational ensemble was used as input in the NAMFIS analysis.

4 Ensemble Analysis Using the Software NAMFIS

Solution ensembles were determined by fitting the experimentally measured distances and coupling constants to those back-calculated for computationally predicted conformations following previously described protocols.[14]

Table S14. Results of the NAMFIS-analyses for peptides **1** and **2** using all distances and couplings.

Peptide **1**		Peptide **2**	
Conf. no.[a]	%Population[b]	Conf. no.[a]	%Population[b]
1	***39***	1	36
2	***19***	2	14
3	8	***3***	***11***
4	8	***4***	***7***
5	6	5	6
6	6	***6***	***6***
7	6	***7***	***5***
8	4	8	4
9	4	9	4
		10	3
		11	2

[a]The structures of the most populated conformations are shown in Figures S10 and S11. Hairpin conformations are indicated by numbers in *italic*. [b]The hairpin population in solution was calculated to 58% for peptide **1** and 29% for peptide **2**.

Table S15. Experimentally determined and back-calculated (NAMFIS) interproton distances (Å) and coupling constants (Hz) for the solution ensemble of peptide **1**.

		Interproton distances (Å)	
Protons		Experimental	Calculated
N10-NH	Q2-NH	3.26	3.73
N10-NH	G1-NH	2.32	2.45
N10-NH	V9-Hα	1.82	2.39
S(Me)3-NH	Q2-NH	2.90	3.44
S(Me)3-NH	Q2-Hα	1.84	2.30
S(Me)3-NH	V4-NH	3.01	3.11
S(Me)3-NH	S8-Hα	3.46	4.34
V4-NH	S(Me)3-Hα	1.87	2.34
G6-NH	A7-NH	2.21	2.56
V9-NH	G1-NH	2.98	3.61
V9-NH	S8-Hα	1.85	2.37
V9-NH	S8-NH	2.88	3.08
S8-NH	A7-NH	2.91	2.89
S8-NH	A7-Hα	1.90	2.39
S8-NH	S(Me)3-Hα	3.37	3.63
G1-NH	Q2-Hα	3.30	4.61
G1-NH	S8-Hα	3.49	3.99
G1-NH	N10-Hα	2.23	2.69
G1-NH	V9-Hα	2.86	4.22
G1-NH	Q2-NH	2.20	2.24
A7-NH	S(Me)3-Hα	3.22	4.43
A7-NH	S8-Hα	3.66	4.81
Q2-NH	V9-Hα	3.43	4.54
Q2-NH	S(Me)3-Hα	3.66	4.75
Q2-NH	S8-Hα	2.91	3.89
Q2-NH	N10-Hα	3.24	4.28
S8-Hα	S(Me)3-Hα	2.18	2.34
S8-Hα	A7-Hα	3.18	4.53
S8-Hα	Q2-Hα	4.06	3.32
S(Me)3-Hα	Q2-Hα	3.00	4.49
	RMS deviation of distances:		*0.80*
		Coupling constants	
Protons		Experimental	Calculated
S8-Hα	S8-NH	9.0	8.0
S(Me)3-Hα	S(Me)3-NH	7.7	8.2
V9-Hα	V9-NH	8.9	8.1
N10-Hα	N10-NH	7.7	8.2
A7-Hα	A7-NH	9.1	8.1
Q2-Hα	Q2-NH	9.7	8.7
	RMS deviation of couplings:		*0.85*

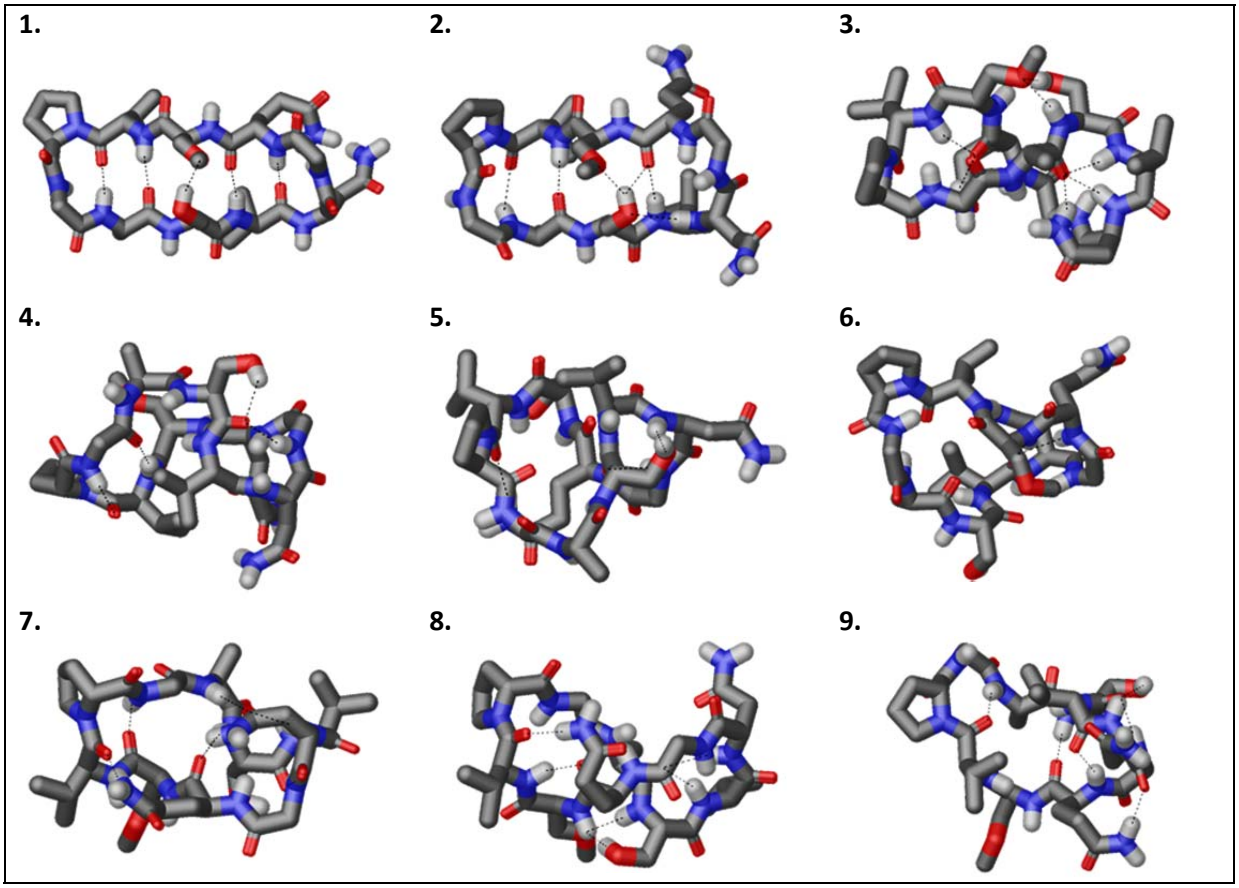

Figure S10. The most populated solution conformations of peptide **1**, as selected by the NAMFIS-analysis. Populations in % are given in Table S14. Hydrogen bonds are indicated by dotted lines. Non-polar (CH) hydrogens are omitted for clarity.

Table S16. Experimentally determined and back-calculated (NAMFIS) interproton distances (Å) and coupling constants (Hz) for the solution ensemble of peptide **2**.

		Inter proton distances (Å)	
Protons		Experimental	Calculated
N10-NH	G1-NH	2.28	2.72
N10-NH	V9-Hα	1.78	2.53
N10-NH	Q2-NH	3.20	3.52
N10-NH	V9-NH	2.90	2.72
S(Me)3-NH	X8-Hα	3.25	4.63
S(Me)3-NH	Q2-Hα	1.81	2.31
S(Me)3-NH	V4-NH	2.97	2.74
S(Me)3-NH	Q2-NH	2.93	3.26
S(Me)3-NH	V9-NH	3.67	5.10
V4-NH	S(Me)3-Hα	1.83	2.53
V4-NH	V9-NH	2.91	4.17
V4-NH	X8-Hα	2.38	3.07
V4-NH	A7-Hα	3.34	4.43
G6-NH	A7-NH	2.15	2.45
G6-NH	^{D}P5-Hα	1.98	2.32
V9-NH	S(Me)3-Hα	2.51	3.54
V9-NH	X8-Hα	1.77	2.24
V9-NH	Q2-Hα	3.43	5.06
V9-NH	Q2-NH	2.37	3.04
V9-NH	G1-NH	3.11	4.07
X8-NH	A7-NH	3.08	3.04
X8-NH	A7-Hα	1.89	2.43
G1-NH	V9-Hα	2.84	3.86
G1-NH	N10-Hα	2.17	3.00
G1-NH	Q2-NH	2.23	2.24
A7-NH	S(Me)3-Hα	3.24	4.64
A7-NH	X8-Hα	3.67	4.95
Q2-NH	V9-Hα	3.36	4.43
Q2-NH	N10-Hα	3.21	4.45
Q2-NH	S(Me)3-Hα	3.58	4.83
Q2-NH	X8-Hα	2.87	4.08
X8-Hα	S(Me)3-Hα	2.15	2.38
S(Me)3-Hα	Q2-Hα	2.98	4.49
	RMS deviation of distances:		*0.92*
		Coupling constants	
Protons		Experimental	Calculated
X8-Hα	X8-NH	7.3	7.6
S(Me)3-Hα	S(Me)3-NH	7.7	7.8
V9-Hα	V9-NH	8.7	8.5
N10-Hα	N10-NH	6.1	7.1
A7-Hα	A7-NH	9.3	8.3
Q2-Hα	Q2-NH	9.7	8.9
	RMS deviation of couplings:		*0.68*

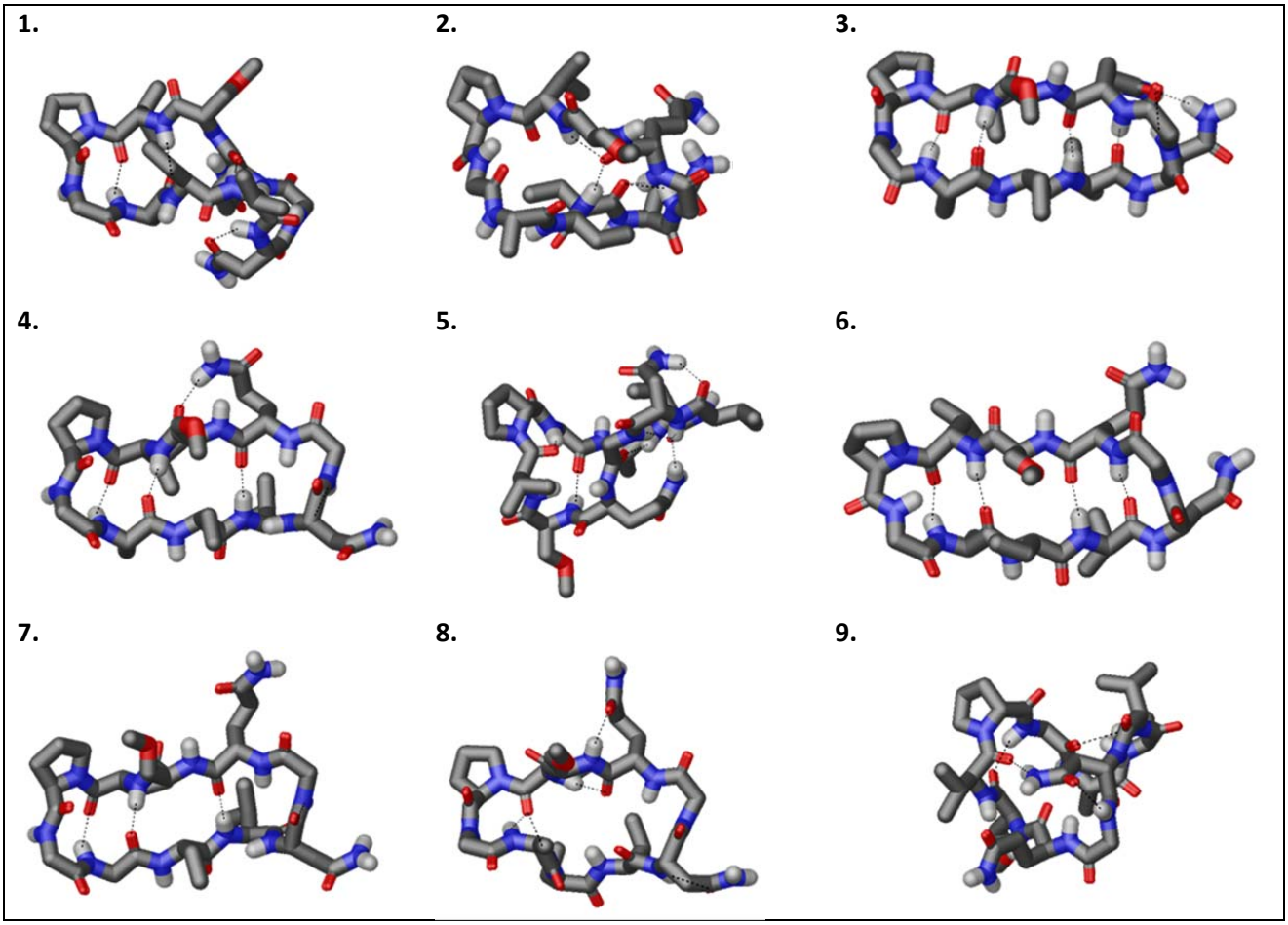

Figure S11. The most populated solution conformations of peptide **2**, as selected by the NAMFIS-analysis. Populations in % are given in Table S14. Hydrogen bonds are indicated by dotted lines. Non-polar (CH) hydrogens are omitted for clarity.

Table S17. Results of the NAMFIS-analyses for peptides **1** and **2** using distances and couplings involving A7.

Peptide **1**		Peptide **2**	
Conf. no.[a]	%Population[b]	Conf. no.[a]	%Population[b]
1	68	***1***	***33***
2	27	***2***	***25***
3	5	3	18
		4	9
		5	9
		6	***6***

[a]The structures of the most populated conformations are shown in Figures S12 and S13. Hairpin conformations are indicated by numbers in *italic*. [b]The hairpin population in solution was calculated to 0% for **1** and 64% for **2**.

Table S18. Experimentally determined and back-calculated (NAMFIS) interproton distances (Å) and coupling constants (Hz) for the solution ensemble of peptide **1**, when the distances and coupling involving A7 were used.

		Interproton distances (Å)	
Protons		Experimental	Calculated
A7-Hβ	V4-NH	2.93	4.09
G6-NH	A7-NH	2.21	2.27
A7-NH	V4-Hβ	3.18	4.16
A7-NH	^{D}P5-Hα	2.80	3.41
A7-Hβ	V4-Hα	3.77	5.31
V4-Hβ	A7-Hβ	2.68	4.03
	RMS deviation of distances:		1.07
		Coupling constants	
Protons		Experimental	Calculated
A7-Hα	A7-NH	9.7	8.9
	RMS deviation of couplings:		*0.77*

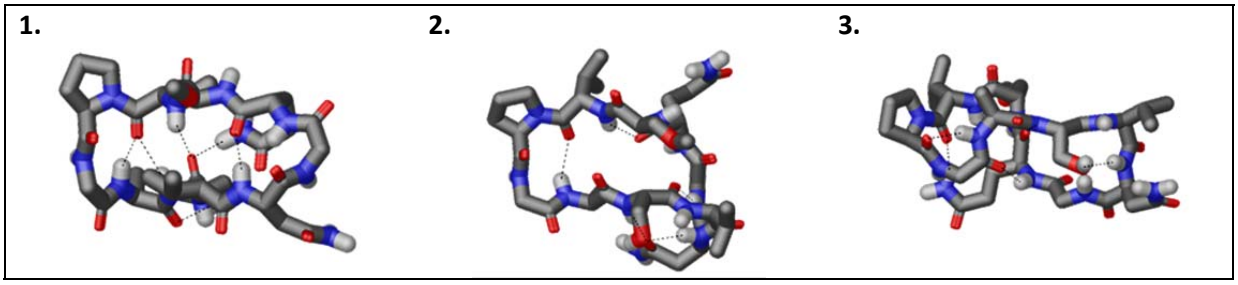

Figure S12. The most populated solution conformations of peptide **1**, as selected by the NAMFIS-analysis, when only the experimental data involving A7 were used. Populations in % are given in Table S17. Hydrogen bonds are indicated by dotted lines. Non-polar (CH) hydrogens are omitted for clarity.

Table S19. Experimentally determined and back-calculated (NAMFIS) interproton distances (Å) and coupling constants (Hz) for the solution ensemble of peptide **2**, when the distances and coupling involving A7 were used.

		Interproton distances (Å)	
Protons		Experimental	Calculated
A7-Hβ	V4-NH	3.02	3.24
V4-NH	A7-Hα	3.34	3.79
G6-NH	A7-NH	2.15	2.30
A7-NH	V4-Hβ	3.10	3.76
A7-Hβ	V4-Hβ	2.72	2.93
	RMS deviation of distances:		0.39
		Coupling constants	
Protons		Experimental	Calculated
A7-Hα	A7-NH	9.3	8.6
	RMS deviation of couplings:		*0.73*

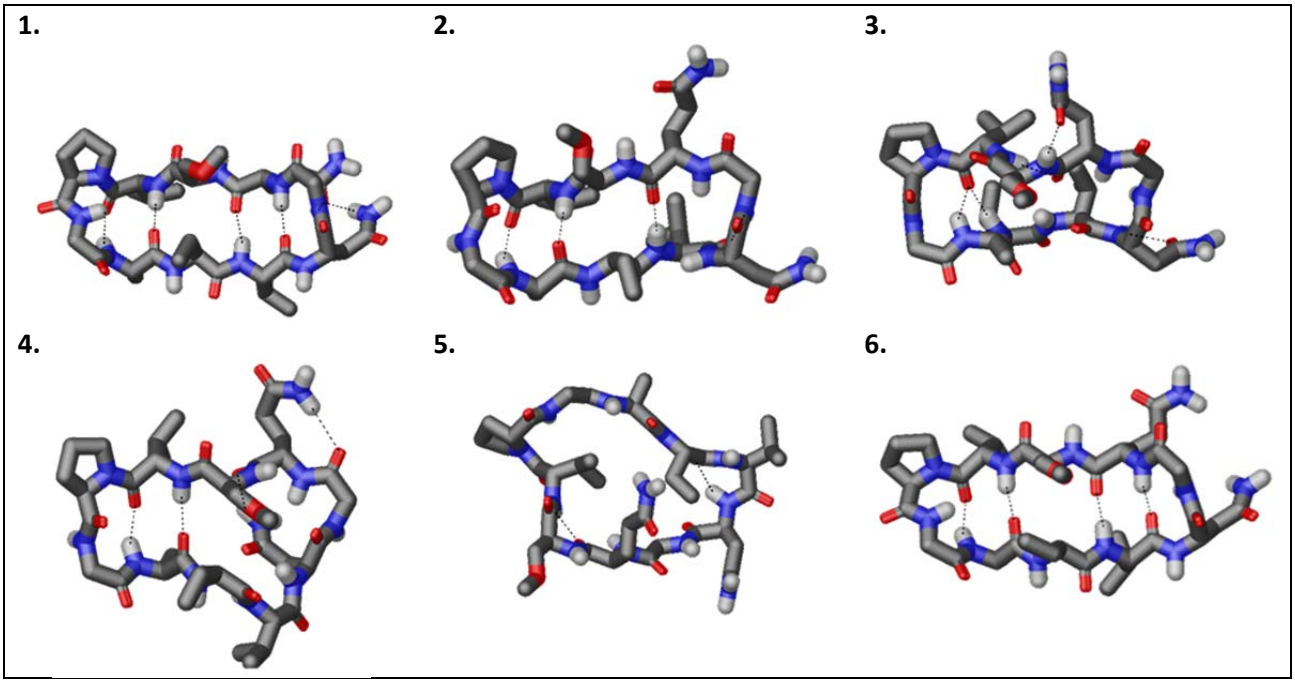

Figure S13. The most populated solution conformations of peptide **2**, as selected by the NAMFIS-analysis, when only the experimental data involving A7 were used. Populations in % are given in Table S17. Hydrogen bonds are indicated by dotted lines. Non-polar (CH) hydrogens are omitted for clarity.

5 MD Simulations

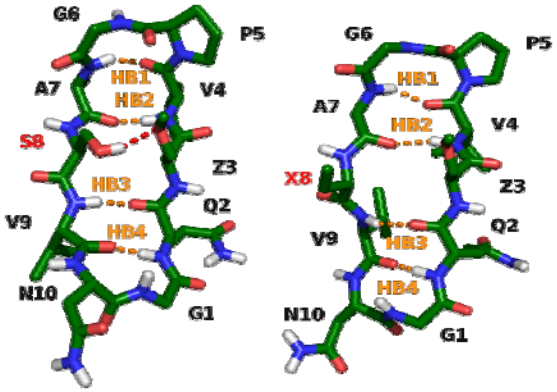

Figure S14. 3D structures of peptides **1** (left) and **2** (right).

Table S20. Conformations with the possible variations of intramolecular hydrogen bond patterns for **1** and **2**, and the corresponding average distances. The first column contains a classification of the hydrogen bonds HB1–HB4 (Figure S14), where *o* stand for open and *c* stand for closed. Structures having hydrogen bond patterns with three and more closed backbone hydrogen bonds are defined as folded (f), whereas those with less than three are defined as unfolded (u).

		Average distances (Å)					
H-bonds	%	HB1	HB2	HB3	HB4	Average	Folded?
Peptide **1**							
Oooo	9	6.23	9.29	7.78	4.15	6.87	u
Oooc	9	5.00	6.96	5.11	2.38	4.86	u
Cooc	13	2.35	3.35	4.04	2.21	2.99	u
Cocc	19	2.36	3.49	2.16	2.17	2.54	f
Ccoc	7	2.20	2.39	3.83	2.24	2.67	f
Cccc	35	2.23	2.06	2.07	2.23	2.15	f
Oocc	2	3.20	3.86	2.19	2.17	2.85	u
Cooo	1	2.41	4.36	5.32	4.67	4.19	u
Ccco	2	2.20	1.98	2.18	3.81	2.54	f
Ccoo	2	2.14	2.18	4.00	4.30	3.15	u
Coco	0	2.37	3.53	2.29	3.21	2.85	u
Occc	1	2.90	2.09	2.04	2.22	2.31	f
Ococ	0	2.90	2.53	3.88	2.19	2.88	u
Ooco	0	3.27	3.83	2.25	3.30	3.16	u
Occo	0	2.89	2.06	2.15	3.81	2.73	u
Ocoo	0	2.97	2.37	4.50	5.06	3.72	u
Folded	**64%**						
unfolded	36%						
Peptide **2**							
Oooo	25	6.18	8.43	7.41	5.08	6.77	u
Oooc	7	5.27	7.63	5.43	2.47	5.20	u
Cooc	21	2.30	3.26	4.02	2.19	2.94	u
Cocc	12	2.34	3.29	2.23	2.16	2.51	f
Ccoc	12	2.19	2.40	3.90	2.21	2.67	f
Cccc	16	2.23	2.13	2.12	2.25	2.18	f
Oocc	1	3.66	4.16	2.27	2.17	3.07	u
Cooo	1	2.53	5.26	5.95	5.07	4.70	u
Ccco	2	2.21	1.98	2.10	4.12	2.60	f
Ccoo	1	2.09	2.20	3.97	3.60	2.96	u
Coco	0	2.34	3.42	2.34	3.20	2.82	u
Occc	0	2.94	2.16	2.05	2.26	2.35	f
Ococ	0	2.94	2.55	3.87	2.18	2.89	u
Ooco	0	3.91	4.18	2.41	3.23	3.43	u
Occo	0	2.94	2.04	2.05	4.44	2.87	u
Ocoo	0	2.80	2.37	3.92	3.55	3.16	u
Folded	**43%**						
Unfolded	57%						

Table S21. Full population (%) change maps for the seven most populated groups of peptide **1**. The hydrogen bonds HB1–HB4 (Figure S14) are denoted by *c* for closed (i.e. HB criteria met) and *o* for open (i.e. HB criteria not met). The most probable folding pathway is indicated by the highest values in respective rows, ignoring the diagonal value.

Peptide **1**																
	To															
From	*oooo*	*oooc*	*cooc*	*cocc*	*ccoc*	*cccc*	*oocc*	*cooo*	*ccco*	*ccoo*	*coco*	*occc*	*ococ*	*ooco*	*occo*	*ocoo*
oooo	**89**	**10**	0	0	0	0	0	**1**	0	0	0	0	0	0	0	0
oooc	**10**	**78**	**9**	**1**	**2**	0	**1**	0	0	0	0	0	0	0	0	0
cooc	0	**6**	**64**	**8**	**17**	**3**	**1**	**1**	0	0	0	0	0	0	0	0
cocc	0	0	**6**	**72**	**1**	**15**	**4**	0	0	0	**1**	0	0	0	0	0
ccoc	0	**2**	**32**	**4**	**47**	**9**	0	0	0	**4**	0	0	**1**	0	0	0
cccc	0	0	**1**	**8**	**2**	**83**	**1**	0	**3**	0	0	**3**	0	0	0	0
oocc	0	**3**	**5**	**49**	**1**	**13**	**26**	0	0	0	0	2	0	0	0	0
cooo	**11**	**2**	**16**	**1**	**3**	0	0	**59**	0	**8**	0	0	0	0	0	0
ccco	0	0	0	**1**	**1**	**40**	0	**0**	**50**	**5**	0	**1**	0	0	**1**	0
ccoo	**1**	0	**1**	0	**16**	**5**	0	**4**	**6**	**66**	0	0	0	0	0	**2**
coco	0	0	**3**	**63**	**1**	**14**	**4**	**1**	**2**	0	**9**	0	0	**1**	0	0
occc	0	0	**1**	**4**	**1**	**79**	**2**	0	**2**	0	0	**11**	0	0	0	0
ococ	0	**11**	**29**	**3**	**39**	**7**	**1**	0	0	**2**	0	**1**	**6**	0	0	0
ooco	**2**	**1**	**1**	**27**	**1**	**17**	**28**	**1**	**5**	0	**8**	**3**	0	**7**	**2**	0
occo	0	0	0	**1**	**1**	**36**	**1**	0	**45**	**3**	0	**5**	0	0	**6**	0
ocoo	**5**	0	**1**	0	**7**	**3**	0	**3**	**4**	**65**	0	0	0	0	0	**12**

Table S22. Full population (%) change maps for the seven most populated groups of peptide **2**. The hydrogen bonds HB1–HB4 (Figure S14) are denoted by c for closed (i.e. HB criteria met) and o for open (i.e. HB criteria not met). The most probable folding pathway is indicated by the highest values in respective rows, ignoring the diagonal value.

Peptide **2**																
	To															
From	*oooo*	*oooc*	*cooc*	*cocc*	*ccoc*	*cccc*	*oocc*	*cooo*	*ccco*	*ccoo*	*coco*	*occc*	*ococ*	*ooco*	*occo*	*ocoo*
oooo	**94**	**5**	0	0	0	0	0	**1**	0	0	0	0	0	0	0	0
oooc	**17**	**72**	**7**	**1**	**2**	0	**1**	0	0	0	0	0	0	0	0	0
cooc	0	**2**	**68**	**5**	**21**	**3**	0	**1**	0	0	0	0	0	0	0	0
cocc	0	0	**9**	**65**	**3**	**17**	**3**	0	0	0	**1**	0	0	0	0	0
ccoc	0	**1**	**35**	**2**	**52**	**5**	0	0	0	**3**	0	0	**1**	0	0	0
cccc	0	0	**3**	**12**	**4**	**73**	**1**	0	**3**	0	0	**2**	0	0	0	0
oocc	0	**4**	**4**	**35**	**1**	**11**	**42**	0	0	0	0	**1**	0	0	0	0
cooo	**21**	**1**	**13**	**1**	**2**	0	0	**57**	0	**4**	0	0	0	0	0	0
ccco	0	0	0	**1**	**1**	**31**	0	0	**60**	**3**	0	**1**	0	0	**2**	0
ccoo	0	0	**2**	0	**24**	**4**	0	**4**	**3**	**61**	0	0	0	0	0	0
coco	0	0	**4**	**61**	**1**	**15**	**3**	**2**	**3**	0	**9**	0	0	**1**	0	0
occc	0	0	**1**	**7**	**2**	**73**	**3**	0	**3**	0	0	**10**	0	0	0	0
ococ	0	**7**	**32**	**3**	**46**	**5**	**1**	0	0	**1**	0	0	**4**	0	0	0
ooco	**5**	**6**	**1**	**26**	**1**	**12**	**32**	**2**	**7**	**1**	**1**	**2**	0	**5**	0	0
occo	0	0	0	0	0	**26**	**1**	0	**59**	**2**	0	**3**	0	0	**8**	0
ocoo	**3**	0	**1**	**1**	**26**	**4**	0	**7**	**5**	**48**	0	0	0	0	**1**	**3**

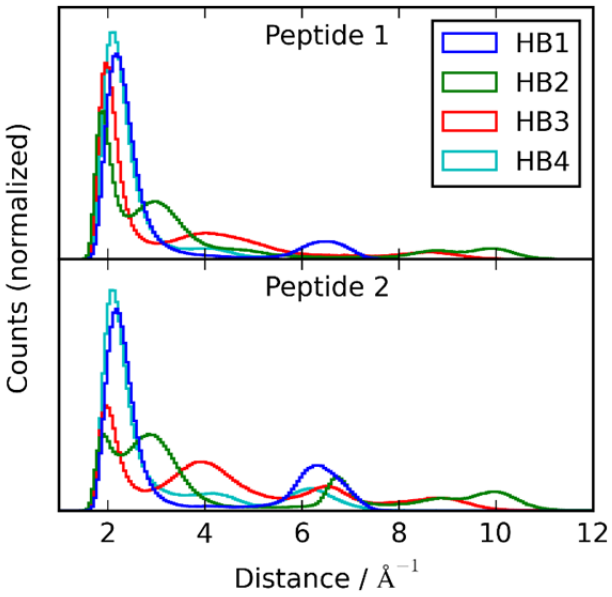

Figure S15. Histograms for hydrogen bond distances HB1–HB4 for **1** and **2**. The replacement of serine (hydrogen bond donor) for 2-aminobutyric acid in position 3 results in longer distances for HB2 and HB3 in the MD simulations, while the turns are not affected.

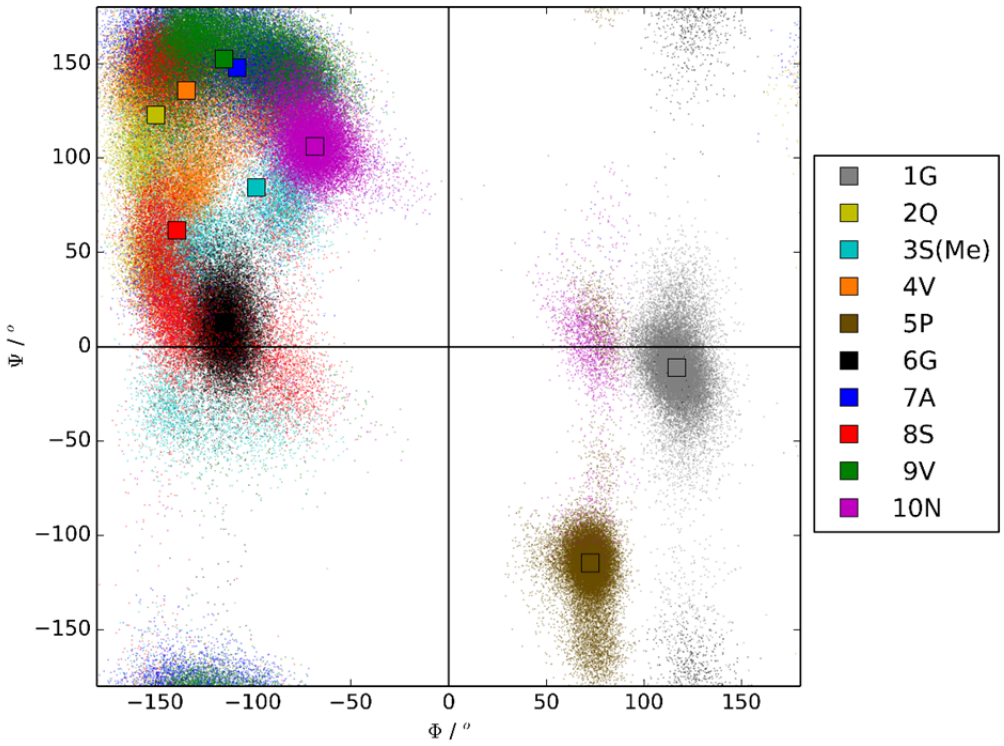

Figure S16. Ramachandran plot for peptide **1**. The ^{D}P5-G6 residues (in brown and black, respectively) were found to induce a type II′ β-turn and the N10-G1 residues (in magenta and grey, respectively) a type II turn. Typical average values of the ϕ and ψ dihedral angles for a type II′ β-turns are $\phi_{i+1} = 60°$, $\psi_{i+1} = -120°$, $\phi_{i+2} = -80°$ and $\psi_{i+2} = 0°$.[15-16] Type II β-turns show the same values but of opposite sign. Each dot represents one structure in the MD trajectory. Only every 100th structure was taken; otherwise the plot becomes too crowded. The squares represent the median of the respective dihedrals. For calculating the median, all values were taken into account.

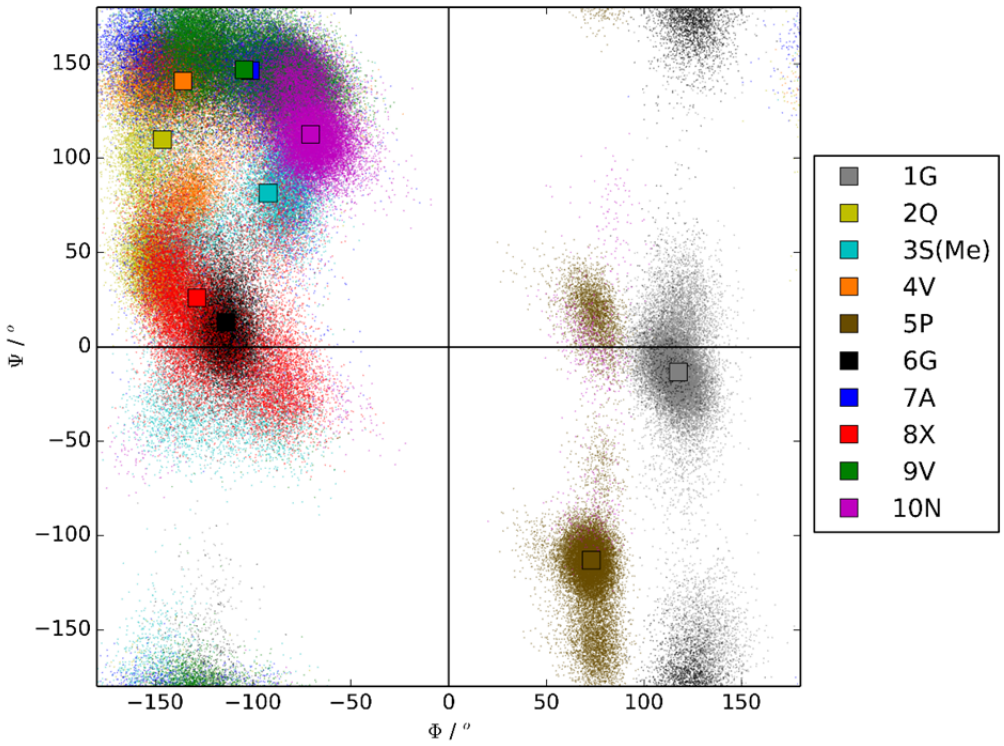

Figure S17. Ramachandran plot for peptide **2**. The ^{D}P5-G6 residues (in brown and black, respectively) were found to induce a type II′ β-turn and the N10-G1 residues (in magenta and grey, respectively) a type II turn.[15-16] For further information see Figure S16 above.

6 Thermodynamic Analysis

A two-state thermodynamic equilibrium between a folded and unfolded conformational ensemble was assumed for the thermal defolding of peptides **1** and **2**.

6.1 Variable Temperature ^{13}C NMR Data — A7-^{13}Cβ Detection

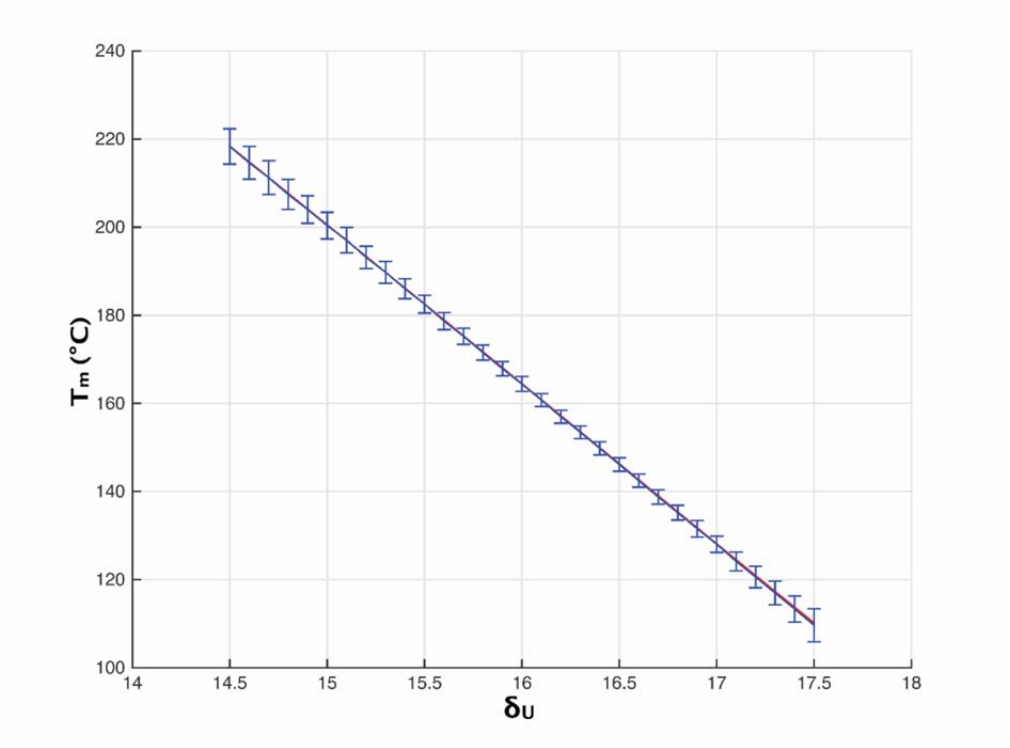

Figure S18. T_m plotted against δ_U for peptide **1**. The error bars represent the standard deviation ranges (±1 SD) of T_m.

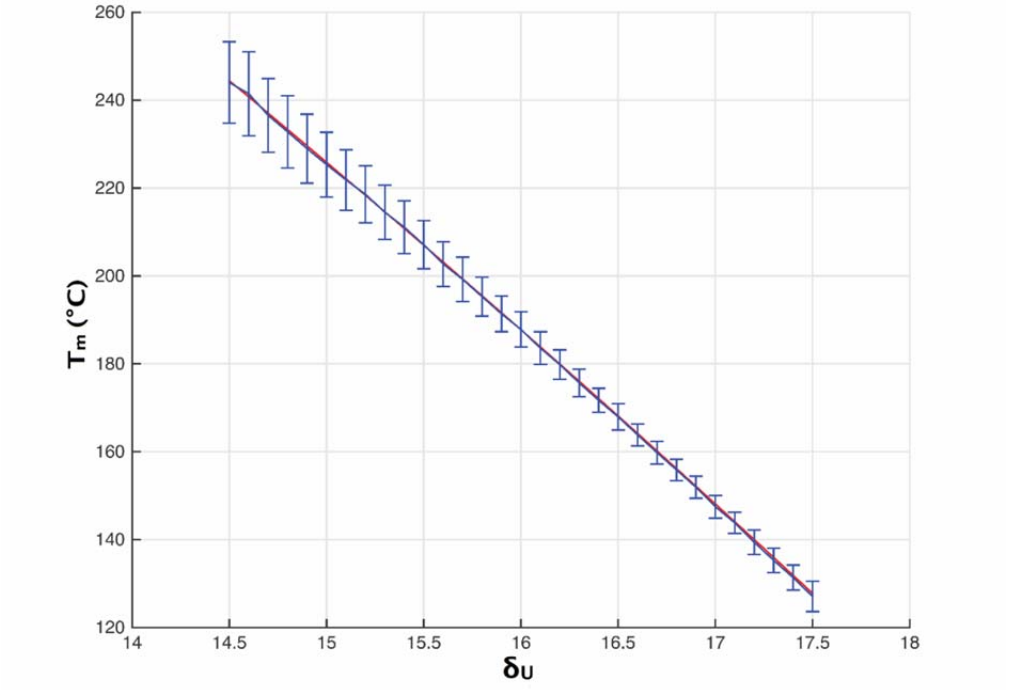

Figure S19. T_m plotted against δ_U for peptide **2**. The error bars represent the standard deviation ranges (±1 SD) of T_m.

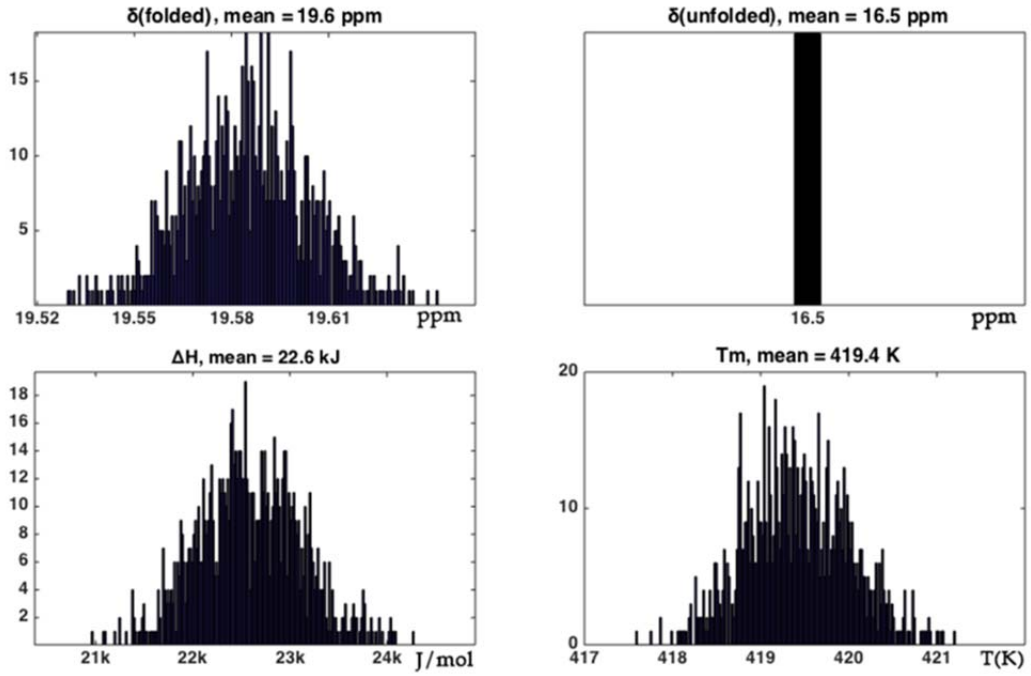

Figure S20. Histogram plots for peptide **1**. Simulated δ_F, ΔH_m and T_m values using a fixed δ_U of 16.5 ppm.

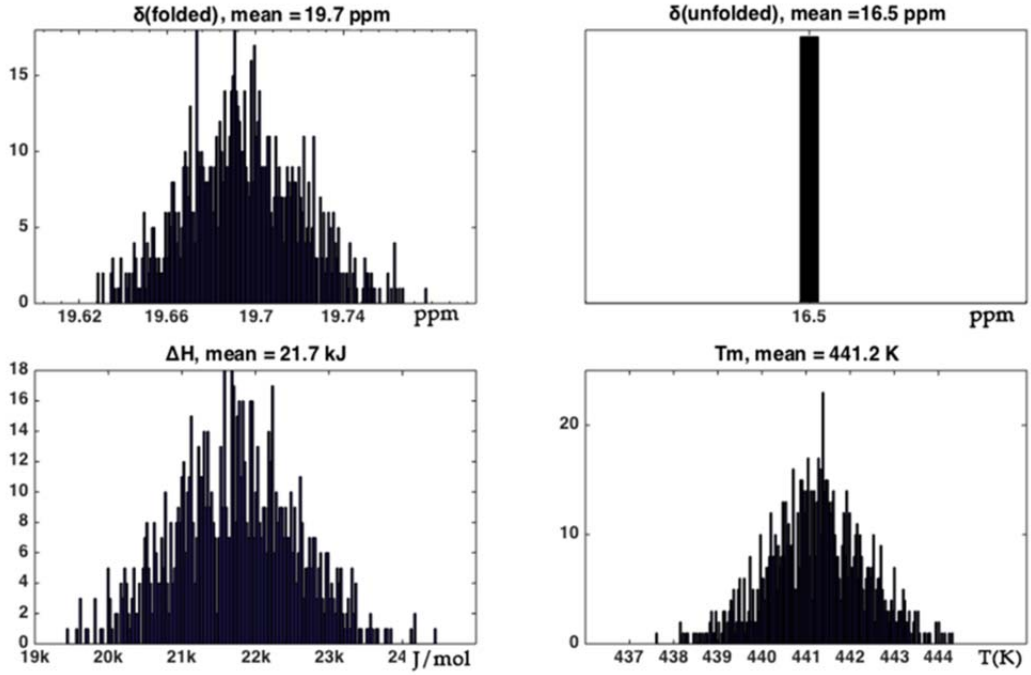

Figure S21. Histogram plots for peptide **2**. Simulated δ_F, ΔH_m and T_m values using a fixed δ_U of 16.5 ppm.

6.2 Variable Temperature ^{13}C NMR Data — ^{13}Cα and ^{13}Cβ Detection

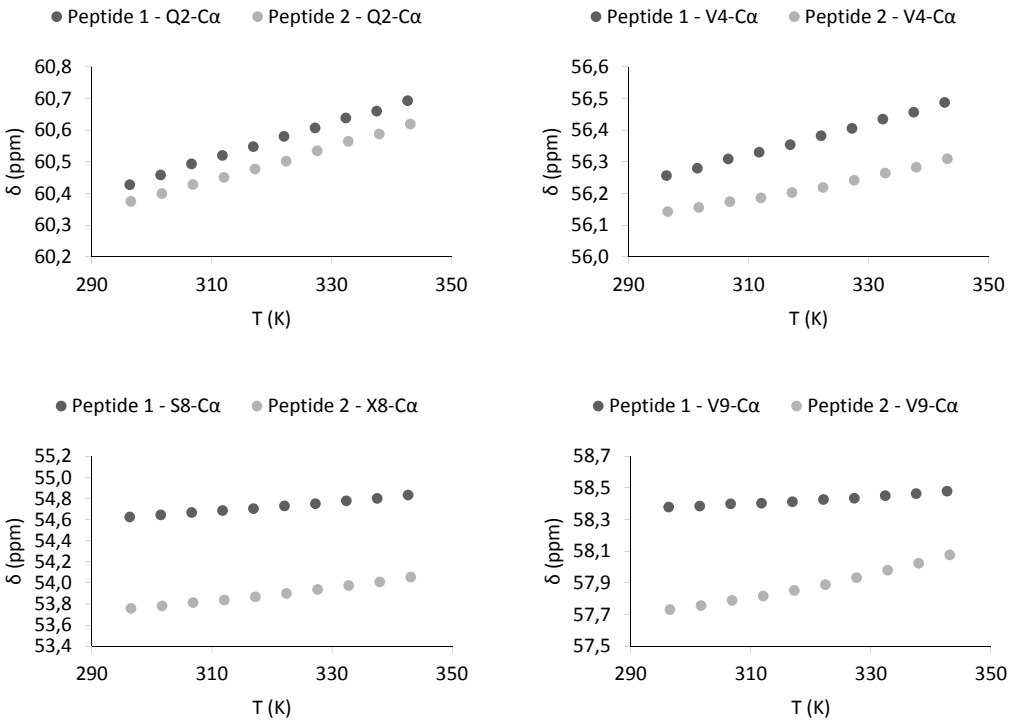

Figure S22. VT ^{13}C NMR data charts for Q2-, V4-, S8/X8- and V9-Cα.

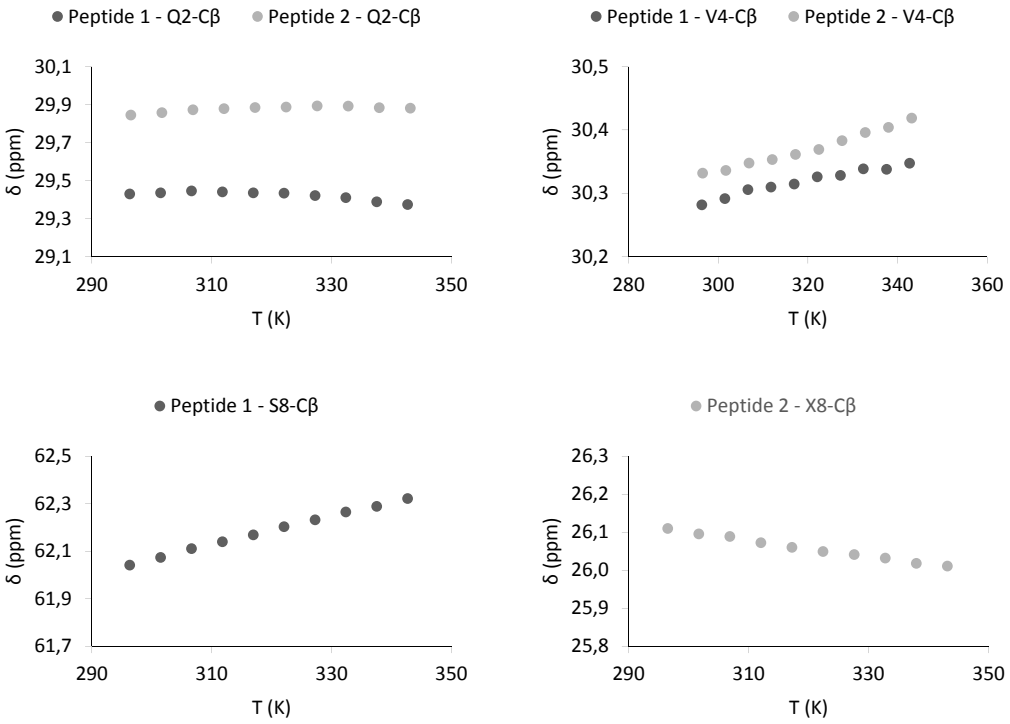

Figure S23. VT ^{13}C NMR data charts for Q2-, V4 - and S8/X8-Cβ.

6.3 Variable Temperature CD Data

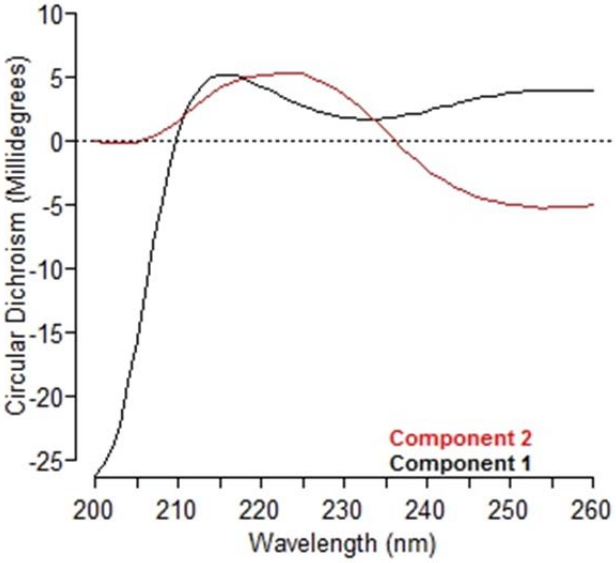

Figure S24. The loadings for components 1 (black) and 2 (red) for the PCA analysis (Figure 4). These show that a gain in component 1 (random coil) is dominated by a gain in random coil, indicated by the negative feature at 200 nm. A gain in component 2 (β-hairpin) indicates a loss of β-turn structure with the broad positive feature at 216–230 nm.

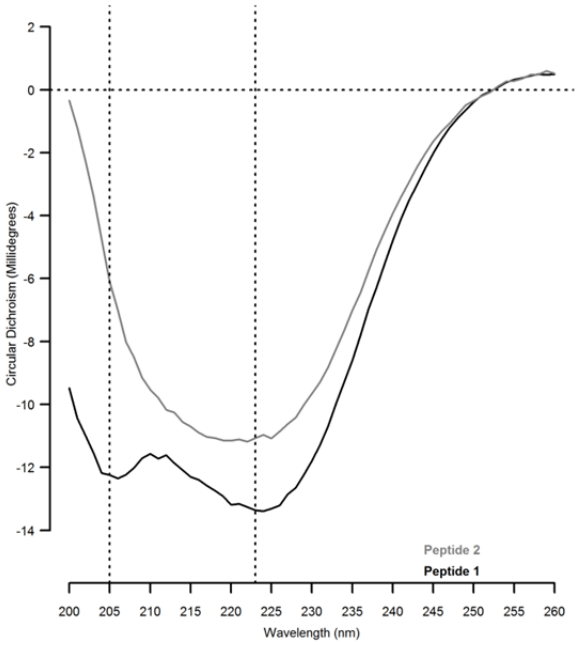

Figure S25. The CD spectra of peptide **1** (black) and **2** (grey) at room temperature. The minima at 205 and 223 nm observed for **1** are typical of a type II′ β-turn, as described by Gibbs *et al*.[17]

7 References

1. The selection of DMSO-d6 as solvent for the NMR studies was based on the limited aqueous solubility of both peptides and the possibility to provide an environment promoting intramolecular hydrogen bonding.
2. Wishart, D. S.; Sykes, B. D.; Richards, F. M., Relationship between nuclear magnetic resonance chemical shift and protein secondary structure. *J. Mol. Biol.* **1991,** *222* (2), 311–333.
3. Yao, J.; Dyson, H. J.; Wright, P. E., Chemical shift dispersion and secondary structure prediction in unfolded and partly folded proteins. *FEBS Lett.* **1997,** *419* (2–3), 285–289.
4. Smith, L. J.; Bolin, K. A.; Schwalbe, H.; MacArthur, M. W.; Thornton, J. M.; Dobson, C. M., Analysis of main chain torsion angles in proteins: prediction of NMR coupling constants for native and random coil conformations. *J. Mol. Biol.* **1996,** *255* (3), 494–506.
5. Andersen, N. H.; Neidigh, J. W.; Harris, S. M.; Lee, G. M.; Liu, Z.; Tong, H., Extracting information from the temperature gradients of polypeptide NH chemical shifts. 1. The importance of conformational averaging. *J. Am. Chem. Soc.* **1997,** *119* (36), 8547–8561.
6. Cierpicki, T.; Otlewski, J., Amide proton temperature coefficients as hydrogen bond indicators in proteins. *J. Biomol. NMR.* **2001,** *21* (3), 249–261.
7. Jiménez, M. A., Design of monomeric water-soluble β-hairpin and β-sheet peptides. In *Protein Design: Methods and Applications*, Köhler, V., Ed. Springer: New York, 2014; Vol. 1216, pp 15–52.
8. Wüthrich, K.; Billeter, M.; Braun, W., Polypeptide secondary structure determination by nuclear magnetic resonance observation of short proton-proton distances. *J. Mol. Biol.* **1984,** *180* (3), 715–740.
9. Spera, S.; Bax, A., Empirical correlation between protein backbone conformation and Cα and Cβ ^{13}C nuclear magnetic resonance chemical shifts. *J. Am. Chem. Soc.* **1991,** *113* (14), 5490–5492.
10. Shu, I.; Scian, M.; Stewart, J. M.; Kier, B. L.; Andersen, N. H., ^{13}C structuring shifts for the analysis of model β-hairpins and β-sheets in proteins: diagnostic shifts appear only at the cross-strand H-bonded residues. *J. Biomol. NMR.* **2013,** *56* (4), 313–329.
11. Santiveri, C. M.; Rico, M.; Jiménez, M. A., ^{13}Cα and ^{13}Cβ chemical shifts as a tool to delineate β-hairpin structures in peptides. *J. Biomol. NMR.* **2001,** *19* (4), 331–345.
12. Hoffman, R. E.; Davies, D. B., Temperature dependence of NMR secondary references for D_2O and $(CD_3)_2SO$ solutions. *Magn. Reson. Chem.* **1988,** *26* (6), 523–525.
13. Grathwohl, C.; Wüthrich, K., Carbon-13 NMR of the protected tetrapeptides TFA-Gly-Gly-L-X-L-Ala-OCH_3, where X stands for the 20 common amino acids. *J. Magn. Reson.* **1974,** *13* (2), 217–225.
14. Cicero, D. O.; Barbato, G.; Bazzo, R., NMR analysis of molecular flexibility in solution: a new method for the study of complex distributions of rapidly exchanging conformations. Application to a 13-residue peptide with an 8-residue loop. *J. Am. Chem. Soc.* **1995,** *117* (3), 1027–1033.
15. Richardson, J. S., The anatomy and taxonomy of protein structure. In *Advances in Protein Chemistry*, Anfinsen, C. B.; Edsall, J. T.; Richards, F. M., Eds. Academic Press: New York, 1981; Vol. 34, pp 167–339.
16. Venkatachalam, C. M., Stereochemical criteria for polypeptides and proteins. V. conformation of a system of three linked peptide units. *Biopolymers* **1968,** *6* (10), 1425–1436.
17. Gibbs, A. C.; Bjorndahl, T. C.; Hodges, R. S.; Wishart, D. S., Probing the structural determinants of type II' β-turn formation in peptides and proteins. *J. Am. Chem. Soc.* **2002,** *124* (7), 1203–1213.